



JOINT INSTITUTE FOR NUCLEAR RESEARCH
Veksler and Baldin laboratory of High Energy Physics

FINAL REPORT ON THE START PROGRAMME

Analysis for Fixed Target Mode for the MPD
experiment: Particle Identification

Supervisor

Dr. Ivonne Alicia Maldonado Cervantes

Students

Francisco Reyes
Universidad Nacional
Autonoma de México

Participation period:

June 30 - August 24,
Summer Session 2024

September 1, 2024

Abstract

In this work, simulated data was used in UrQMD for the fixed targeted mode at an energy of $\sqrt{s_{AB}} = 2.9$ GeV with $Xe^{124} + W^{184}$, for the MPD experiment, resolutions of different variables were used to find the ranges, where it was necessary to make different cuts, to clean up the data, finding the following cuts $NHits \geq 20$, $DCA \leq 2$, $\eta \in [-1, 2]$, these are used to find distributions of multiplicity and energy loss, with multiplicity and use of CentralityFramework different kinds of centrality were found, which is planned to be used in the future for different species of particles, with energy loss data, Particle identification was carried out using the Bethe-Bloch equation and p_T efficiency as a corroboration of the particle selection was obtained in the end adequate, although much work remains to be done in the future.

Contents

1	Introduction	2
2	Concept development	2
2.1	MPD experiment in NICA	2
2.2	Generator UrQMD and Framework MpdRoot	4
2.3	Fixed Target Mode	4
2.4	Centrality	4
2.5	Particle identification	5
3	System configuration of Fixed Target Mode	6
4	Code	7
5	Primary Vertex and cuts	7
5.1	Track selection to get Multiplicity distribution	9
6	Implementation of the methods with the Centrality Framework	12
6.1	GammaFit results	12
6.2	Comparison of results	16
7	Particle identification	18
7.1	Energy loss and mass in funcion the p^*q	18
7.2	Fit of data	20
7.3	Sigma and limits	23
7.4	Comparison Fixed Target Mode and Low Magnetic Field	25
7.5	Limits for the dE/dx	27
7.6	p_T Rec and p_T MC and resolution	28
8	Conclusions	31
	Bibliography	32

1 Introduction

The MPD experiment will start taking data in the fixed target configuration by mid-2025. It is therefore necessary to characterize the detector response and obtain some of the global variables such as centrality. In this report we show a preliminary analysis of the centrality classes obtained in collisions $Xe + W$ at $E_{lab} = 2.5 GeV$ ($\sqrt{s_{AB}} = 2.9 GeV$) simulated with the event generator UrQMD. For the analysis we use the multiplicity distribution of tracks reconstructed by the TPC that meet certain selection criteria. We use the GammaFit method of centrality extraction supported by the CentralityFramework [1], software which has already implemented for the MPD experiment.

In the following sections we show the methodology used to accomplish this task. In the section 3 we describe the parameters used in UrQMD to generate $\approx 0.4M$ of events, also we show a preliminary set of cuts, both in the primary vertex and cuts used for track. In the section 7 we explain the parameters implemented to run the Centrality Framework within the NCX cluster[2].

For the work also implemented the identification of particles, by parameterization of energy loss distributions, for different species of particles, in this work a greater focus was given to π^+ , K^+ and p . Finding also the efficiency of p_T from the PID (particle identification) selection described in section 8.

2 Concept development

2.1 MPD experiment in NICA

The mega project NICA (Nuclotron-based Ion Collider fAcility)[3], has the objective of studying the properties of nuclear matter in the region of maximum barionic density, such matter exists only in neutron stars and in the early stages of the universe, In the theoretical part we know calculations of Lattice QCD predict phase transition, for the deconfinement of hadron matter QGP (Quark-Gluon Plasma) in the energies at which the experiment will work [4]. In addition, it is particularly important to determine the critical point of the deconfinement of matter, so that the energy range from $\sqrt{s_{NN}} = 3-11 GeV$ is planned to be studied. NICA also has 3 modes of operation for the study of its objectives, as set out below:

1. Acceleration of heavy ions for storage in the collider.
2. Acceleration of polarized protons and deuterons for feeding the collider.
3. Acceleration of both polarized and unpolarized protons and deuterons and heavy ions for internal target experiments or slow extraction to fixed target experiments.

In the case of the work presented here, the study was carried out on the third mode of operation of the nuclotron, which is called Fixed Target Mode.

The study of reduced magnetic field for collider mode has recently been included, and a brief comparison will be made in section 7.4 on particle identification. The MPD detector (Multi Purpose Detector) was built for the detection of charged hadrons, electrons and photons for high luminosity heavy ions that will have implemented a 3-D tracking and a high performance particle identification (PID) system based on flight time and calorimetry. At design luminosity, the event rate in the MPD interaction region is approximately 6 kHz. It is also assumed that the total multiplicity of charged particles exceeds 1000 in the most central Au+Au collisions at an energy of $\sqrt{s_{NN}} = 11 GeV$ [5].

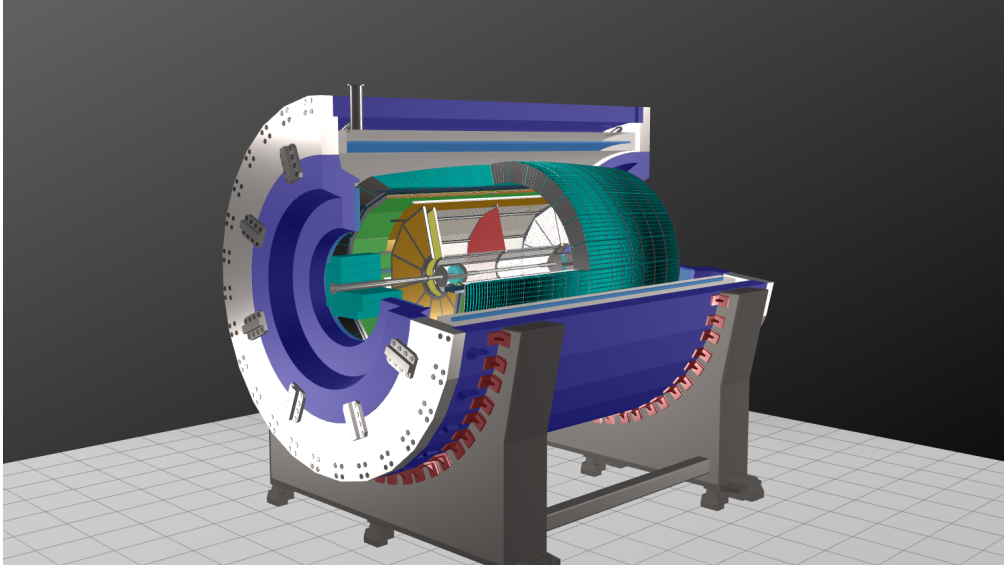


Figure 1: 3-D model MPD detector [6]

The detector consists of the superconducting solenoid, time projection camera (TPC), barrel flight time system (TOF), electromagnetic calorimeter (ECal), zero-degree calorimeter (FHCAL) and fast-forward detector (FFD). Figure 2 shows a diagram of the MPD detector.

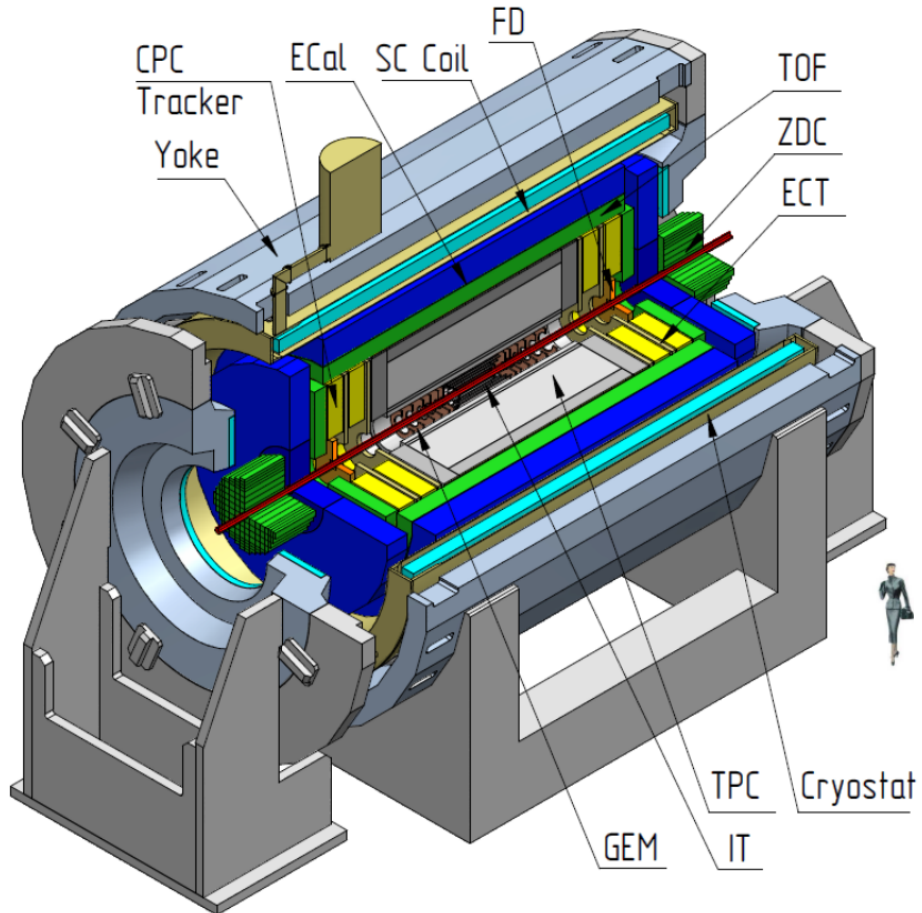


Figure 2: MPD detector and its different components.

2.2 Generator UrQMD and Framework MpdRoot

For the present work we use the event generator of Ultrarelativistic Molecular Dynamics (UrQMD) is a transport model for simulating heavy ion collisions in the energy range from SIS to RHIC which helps to study different physical processes such as multifragmentation and collective flow up to particle production and correlations for generation of events for analysis with the MpdRoot software [7].

The MpdRoot Framework is used for simulation, reconstruction and physical analysis of simulated or experimental data for MPD experiment, for data analysis each specialized analysis wagon is used for certain tasks [8].

2.3 Fixed Target Mode

The fixed-objective experiment is frequently used in physics to generate collision asymmetries, allowing easier disintegrations and giving greater luminosity, These characteristics being a good motivation to be included in the NICA study with QGP and production of strangeness, use in this way will create a wide range of study on little studied phenomena of physics, in the range of energies of the experiment. So it is important to conduct performance and cleanliness studies to make sure that what is measured on the detector is really reliable [9].

2.4 Centrality

In heavy ion collisions experiments the study by centrality classes is of particular importance. The centrality is a calculation that depends on geometric parameters of the collision as is the parameter of impact, also of the total effective section, besides the speed. Centrality can be described as a series of classes where greater centrality (0-10%) is associated with higher production of particles, which is when there is a greater number of participants and collisions inelastically caused by a particular speed [10]. For the centrality study in collisions, multiple methods have been developed, which is used in this work is the GammaFit method using the CentralityFramework software that was previously adapted to the experience in which it is worked [1].

2.4.1 GammaFit

The Bayesian inversion method was proposed by Rudolph Rogly, Giuliano Giacalone and Jean-Yves Ollitrault [11]. The model allows to reconstruct an impact parameter distribution using multiplicity of charged particles without relying on some other external procedure or additional system information collision [1].

In the observable experimental multiplicity we can find that the multiplicity of charged particles (N_{ch}) and the impact parameter (b) are defined by the probability distribution of the charge particles ($P(N_{ch})$).

$$P(N_{ch} | b) = \frac{1}{\Gamma(k)\theta^k} N_{ch}^{k-1} e^{-N_{ch}/\theta} \quad (1)$$

Where $\Gamma(k) \equiv \int_0^\infty x^{k-1} e^{-x} dx$ is the Gamma function and the variables k and θ depend on b and define the multiplication distribution and standard deviation defined as:

$$\langle N_{ch} \rangle = k\theta, \sigma_{N_{ch}} = \sqrt{k\theta} \quad (2)$$

The experimental distribution of produced charged particles can be parametrized using $P(N_{ch} | b)$ over all impact parameters:

$$\frac{1}{M_{\Gamma-fit}} \equiv P(N_{ch}) = \int_0^\infty P(N_{ch} | b)P(b)db, P(b) = \frac{2\pi b}{\sigma_{inel}}P_{inel}(b) \quad (3)$$

Where $\frac{1}{M}$ indicates that the distribution is normalized. $P_{inel}(b)$ is the probability of an inelastic collision occurring on a given b , and σ_{inel} is the inelastic nucleus-nucleus cross section. The variables of b are described in the cumulative probability distribution. c_b

$$c_b = \int_0^b P(b')db' \quad (4)$$

Simplifying the equation is rewritten as:

$$P(N_{ch}) = \int_0^1 P(N_{ch} | b)dc_b \quad (5)$$

Where $P(N_{ch} | b)$ denotes the probability distribution of N_{ch} at fixed c_b , i.e., fixed b . To define the variable k we used the following parameterization:

$$k(b) = k_0 * exp \left(- \sum_{i=1}^3 a_i (c_b)^i \right) \quad (6)$$

With the last equation it is possible to extract different parameters for the use of the method, introducing the Bayes theorem for the calculation of centrality.

$$P(b | N_{ch}^{low} < N_{ch} < N_{ch}^{high}) = P(b) \frac{\int_{N_{ch}^{low}}^{N_{ch}^{high}} P(N_{ch} | b)dN_{ch}}{\int_{N_{ch}^{low}}^{N_{ch}^{high}} P(N_{ch})dN_{ch}} \quad (7)$$

Once the parameters can be extracted with the Bayesian theorem it is possible to make an adjustment to subsequently extract the centrality.

2.5 Particle identification

The loss of energy by ionization is the process by which a charged particle loses energy as it passes through a certain material, in the study of particles this loss of energy is due to the medium that is the detector. This energy loss is crucial for particles identification. By measuring the energy loss (dE/dx), together with the particle moment, you can identify the type of particle and determine its kinetic energy [12]. The theoretical expression predicting ionizing energy loss is the Bethe-Bloch equation, which describes how the energy loss increases proportionally with β^2 as the particle velocity decreases. This equation also takes density into account of the medium through which the particle moves [13].

$$\left\langle -\frac{dE}{dx} \right\rangle = K z^2 \frac{Z}{A} \frac{1}{\beta^2} \left[\frac{1}{2} \log \frac{2m_e c^2 \beta^2 \gamma^2 W_{max}}{I^2} - \beta^2 - \frac{\delta(\beta\gamma)}{2} \right] \quad (8)$$

Where the different variables of the equation are, E is energy, x mass per unit surface, coefficient K for $\frac{dE}{dx}$, z charge number of incident particle, Z atomic number of absorber, A atomic mass of absorber, m_e electron mass, I mean excitation energy, $\delta(\beta\gamma)$ density effect correction to ionization energy loss and W_{max} Maximum possible energy transfer to an electron in a single collision.

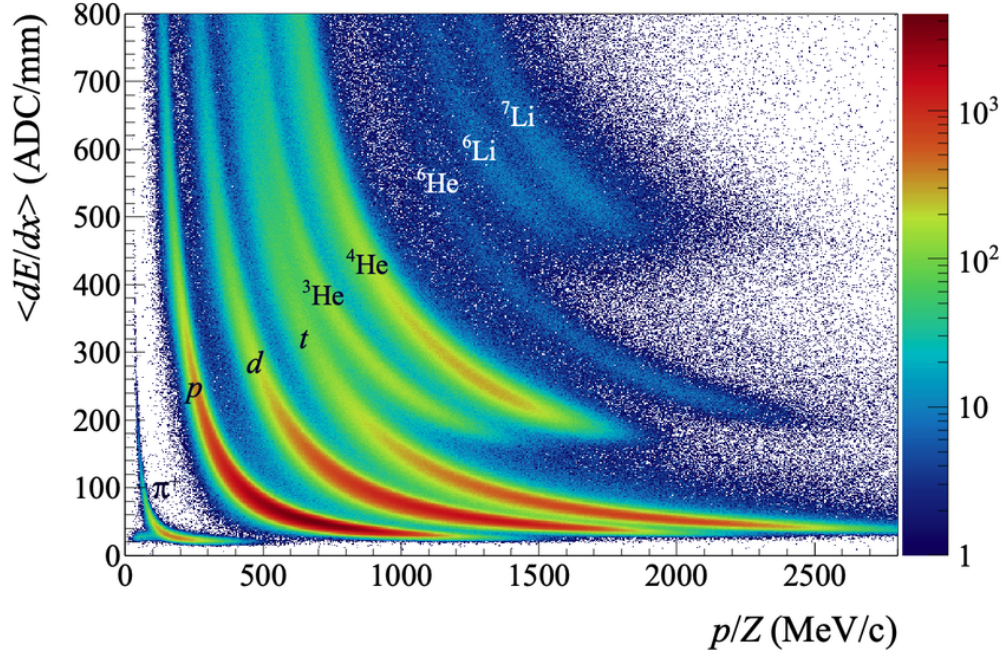


Figure 3: Loss of energy and characterization of different species of particles [14].

Figure 3 shows an example of the energy loss that particles have when passing through a medium.

For the particular case of the MPD in NICA the Bethe-Bloch equation is adjusted as follows where a is a constant p is the total moment [15].

$$\frac{dE}{dx} = \frac{a_0}{\left(\frac{p}{E}\right)^{a_3}} \left(a_1 - \left(\frac{p}{E}\right)^{a_3} \right) - \ln \left(a_2 + \left(\frac{m}{p}\right)^{a_4} \right) \quad (9)$$

3 System configuration of Fixed Target Mode

For our analysis, we simulate 384,800 Xe ($A = 124$) + W collisions at $E_{lab} = 2.5$ GeV using UrQMD (Ultra Relativistic Quark model Dynamics)[16] as a Monte Carlo Event Generator with the following input:

```

pro 124 54           //Projectile Atomic_mass Atomic_number
tar 184 74           //Target Atomic_mass Atomic_number

nev 200              //Number of Events
imp -14.71           //Impact Parameter
ene 2.5              //Kinetic Energy
tim 200 200          //Time

cto 27 1             //Target Mode Option

rsd 16537010         //Random Number
f13
#f14                 //Output File
f15
f16
f19
f20

```

We configure the script `runMC.C` for Fixed Target (FXT) mode setting the variables as appears in the following box:

```
primGen->SetBeam(0.0, 0.0, 1e-6, 1e-6);
primGen->SetTarget(-85.0, 0.0);
primGen->SmearGausVertexZ(kFALSE);
primGen->SmearVertexXY(kFALSE);
```

Finally we process the events with the `runReco.C` script to obtain the `mpddst.root` files. The `mpddst.root` files contain all the information about event and the reconstructed tracks.

4 Code

In this work, a greater focus was given to the physical sense of the analysis, so it was decided that the code should be included in the github platform where each part is described in detail. This can be consulted at the following link:

https://github.com/iamaldonado/START_Summer24/tree/main/FrankReyes

5 Primary Vertex and cuts

In order to find clean distributions background in the data, distributions for primary vertex, impact parameter, pseudorapidity, DCA and Number of Hits were analyzed. The following section describes how distributions were analyzed to make cuts in different variables for more reliable data analysis.

As a first step we analyze the distribution of the z coordinate of the reconstructed primary vertex, shown in figure 4.

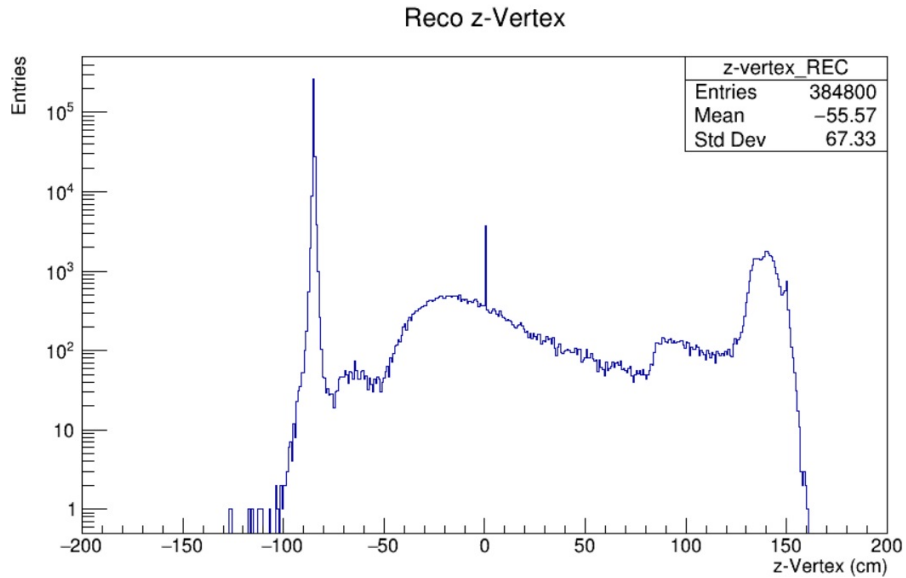


Figure 4: Distribution of z -coordinate of reconstructed primary vertex

The distribution has a peak at $z_{Vertex} = -85.0$ cm, however there are several events in the range -50 cm to 150 cm. To estimate the contribution of the events in this region, we

calculate the percentage of events around the -85 cm peak. The percentage of events with $z_{vertex} \in (-100, -70)$ cm is 80.164% of the total events. To reject these events we apply a cut to the number of generated tracks (MCTracks) obtained after the collision from each event, for the analysis we select events with more than 308 tracks (124 from Xenon and 184 from Wolfram), so we ensure events with more particles than the initial ones. The distribution obtained is shown on figure 5.

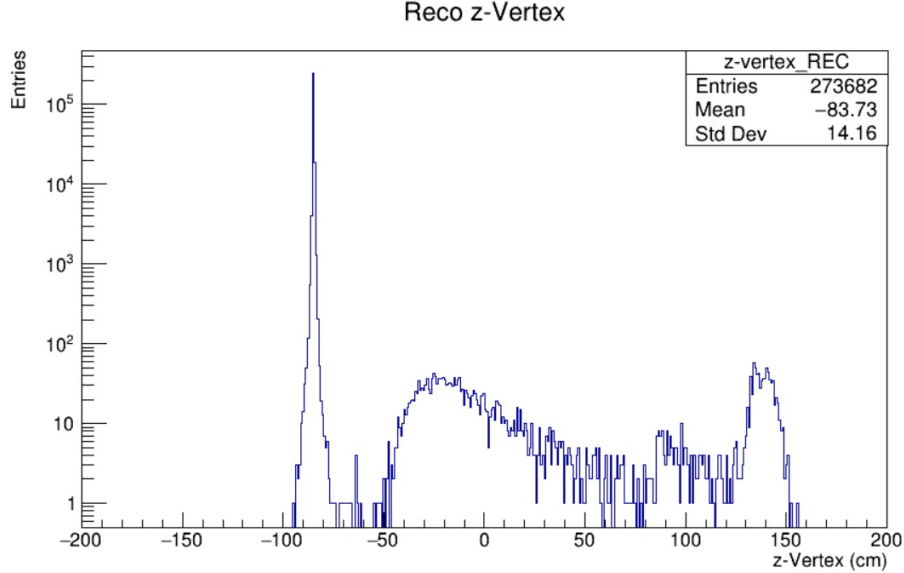


Figure 5: Primary z-Vertex distribution with number of MCTracks higher than 308.

Again we calculate the percentage of events around the -85 cm peak and now it is 98.95% of the total events. We can conclude that contribution of events on $z_{vertex} \in (-50, 150)$ cm is not relevant and can be ignored. Most of the rejected events correspond to peripheral events, as we can see in the distribution of the impact parameter in figure 6. It is important to emphasize that peripheral and low multiplicity events severely affect the reconstruction of the primary vertex ($\Delta z = z - Vertex - z_{MC}$).

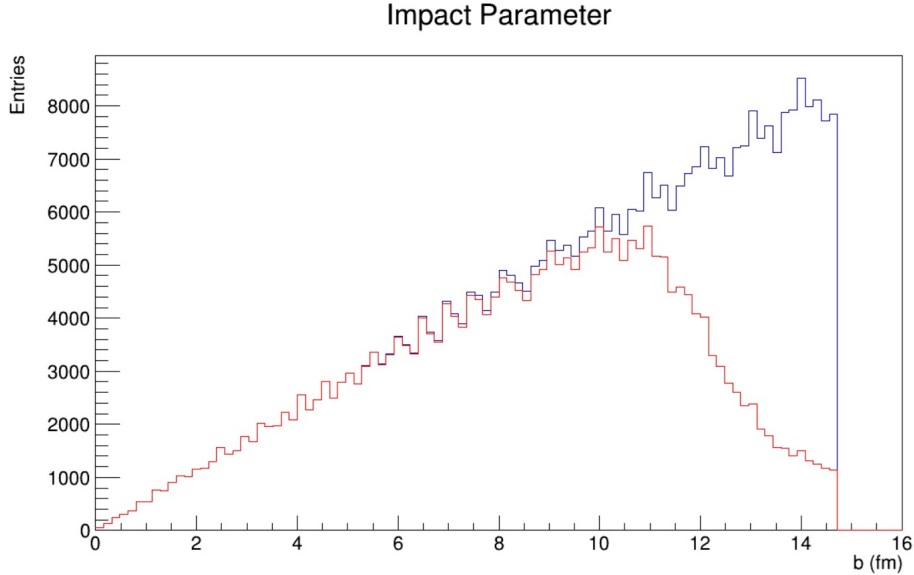


Figure 6: Distribution of the Impact parameter of the events without (blue) cut on the number of MCTracks and with cut (red) on MCTracks > 308.

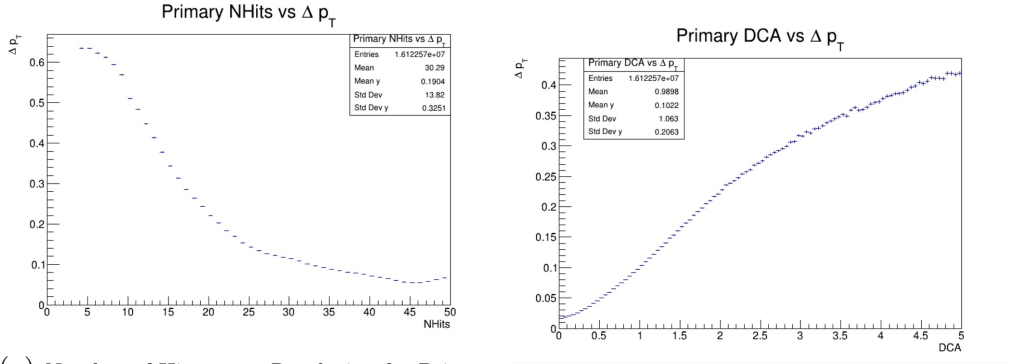
5.1 Track selection to get Multiplicity distribution

To run the centrality Framework we require the multiplicity distribution of reconstructed tracks. To select the tracks, we analyze the transverse momentum resolution

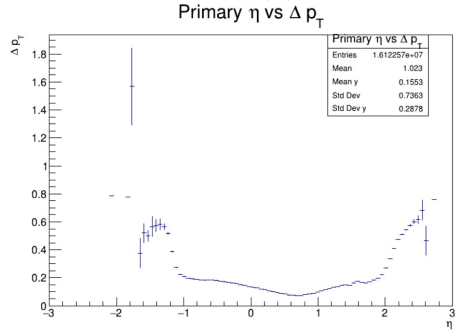
$$\Delta p_T = \frac{|p_T^{Reco} - p_T^{MC}|}{p_T^{MC}} \quad (10)$$

as a function of different variables used to select good reconstructed tracks, as the number of hits in the TPC (Time Projection Chamber), the pseudorapidity η and the DCA (Distance of Closest Approach).

The distribution of Δp_T is shown in the figures 7 and 8 for primary and secondary particles respectively. Besides the cut on pseudorapidity acceptance $-1 < \eta < 2$ we can select events with the $NHits > 20$ and $DCA < 2.0\text{cm}$ to have a transverse momentum resolution below 0.2 for both primary and secondary tracks. Further detailed analysis will be presented later.

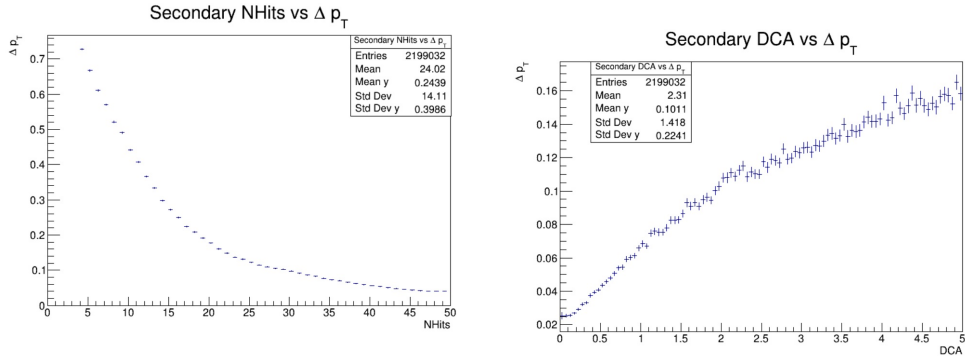


(a) Number of Hits vs p_T Resolution for Primary Particles. (b) DCA vs p_T Resolution for Primary Particles.

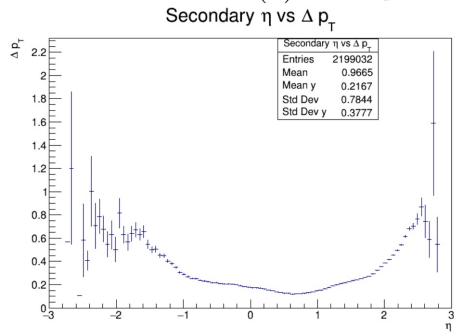


(c) η vs p_T Resolution for Primary Particles.

Figure 7: Primary Particles selected with MC association.



(a) Number of Hits vs p_T Resolution for Secondary Particles. (b) DCA vs p_T Resolution for Secondary Particles.



(c) η vs p_T Resolution for Secondary Particles.

Figure 8: Secondary Particles selected with MC association.

The selected cuts to have a transverse momentum resolution better than 20% are:

1. Number of Hits ≥ 20
2. $DCA \leq 2$
3. $\eta \in [-1,2]$

The comparison of the phase space distribution of reconstructed tracks with and without cuts on impact parameter, Number of Hits, DCA and η , is shown in the figures 9 and 10 for primary and secondary particles respectively. We observe that for primary particles the p_T resolution is too big for particles with $p_T > 2\text{GeV}/c$.

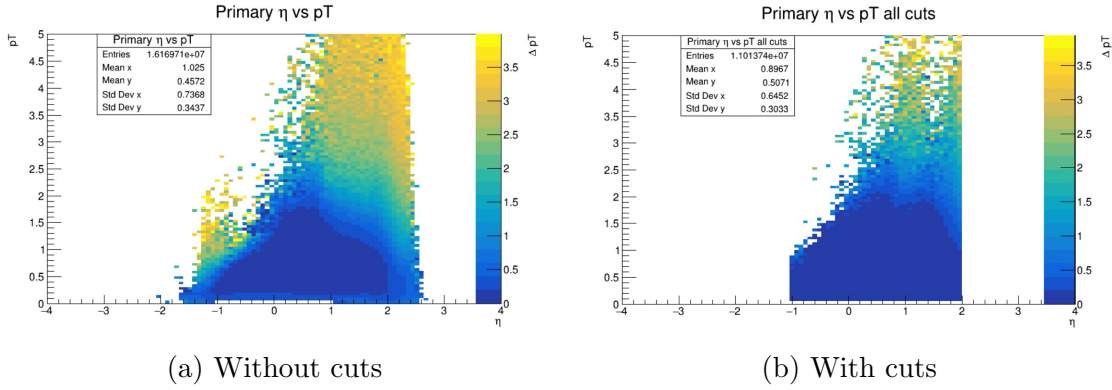


Figure 9: Primary particles η vs p_T resolution, $N_{Hits} \geq 20$, $DCA \leq 2$, $\eta \in [-1, 2]$.

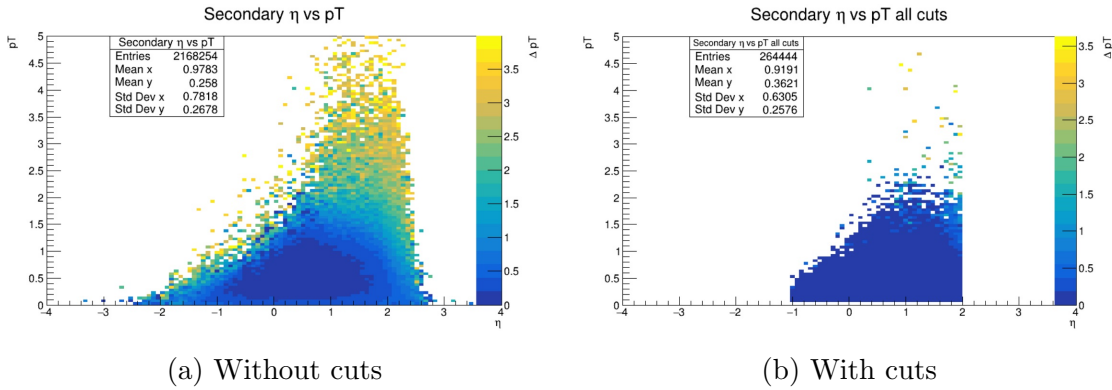


Figure 10: Secondary particles η vs p_T resolution $N_{Hits} \geq 20$, $DCA \leq 2$, $\eta \in [-1, 2]$.

With the previous cuts we obtain the multiplicity distribution, shown in figure 11 that we are going to use to estimate the centrality classes of the events.

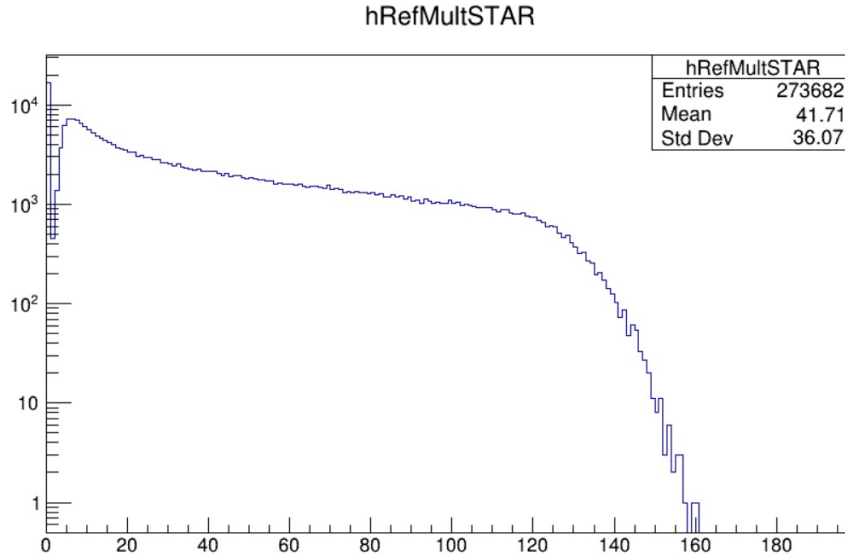


Figure 11: Multiplicity distribution cuts on b , Number of Hits, DCA and η .

6 Implementation of the methods with the Centrality Framework

The cuts made were used to have a cleaner distribution of multiplicity in a histogram, this is used as input information for the software CentralityFramework, which uses the methods GammaFit and MCGLauber, in the stay were used both methods, As a test to see which method works best for the experiment, in this paper we will detail a little more the results of the GammaFit method, since it is the method used for the analysis, although at the end we compare the results with the MCGLauber method. The purpose of finding classes of centrality is to subsequently carry out studies of p_T and multiplicity, by species of particle and by centrality using particle identification. Unfortunately the use of centrality classes could not be realized due to lack of time but it is planned to implement later.

6.1 GammaFit results

For the use of the software is used an input file multiplicity that can be obtained with count of reconstructed tracks , to this one is made a configuration as you can see in figure 12, the right side is the input file and on the left side is the fit made by the software.

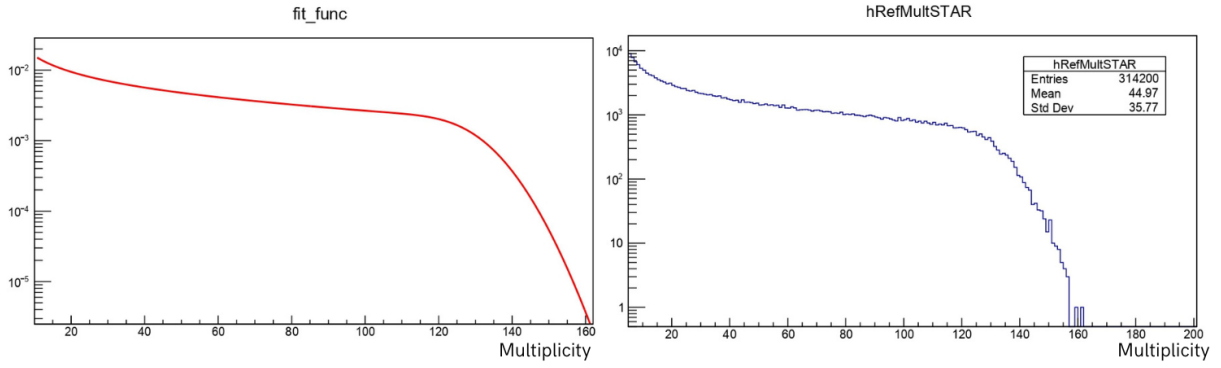


Figure 12: input file multiplicity in blue and red multiplicity adjustment

Below you will find the histograms of the centrality parameter setting impact by centrality compared to that used from the input file.

The figure 13 shows as an example for centrality of 5-10%, 40-50% and 80-100% of the right side are reconstructed from the adjustment and left are calculated from the information provided by the UrQMD generator.

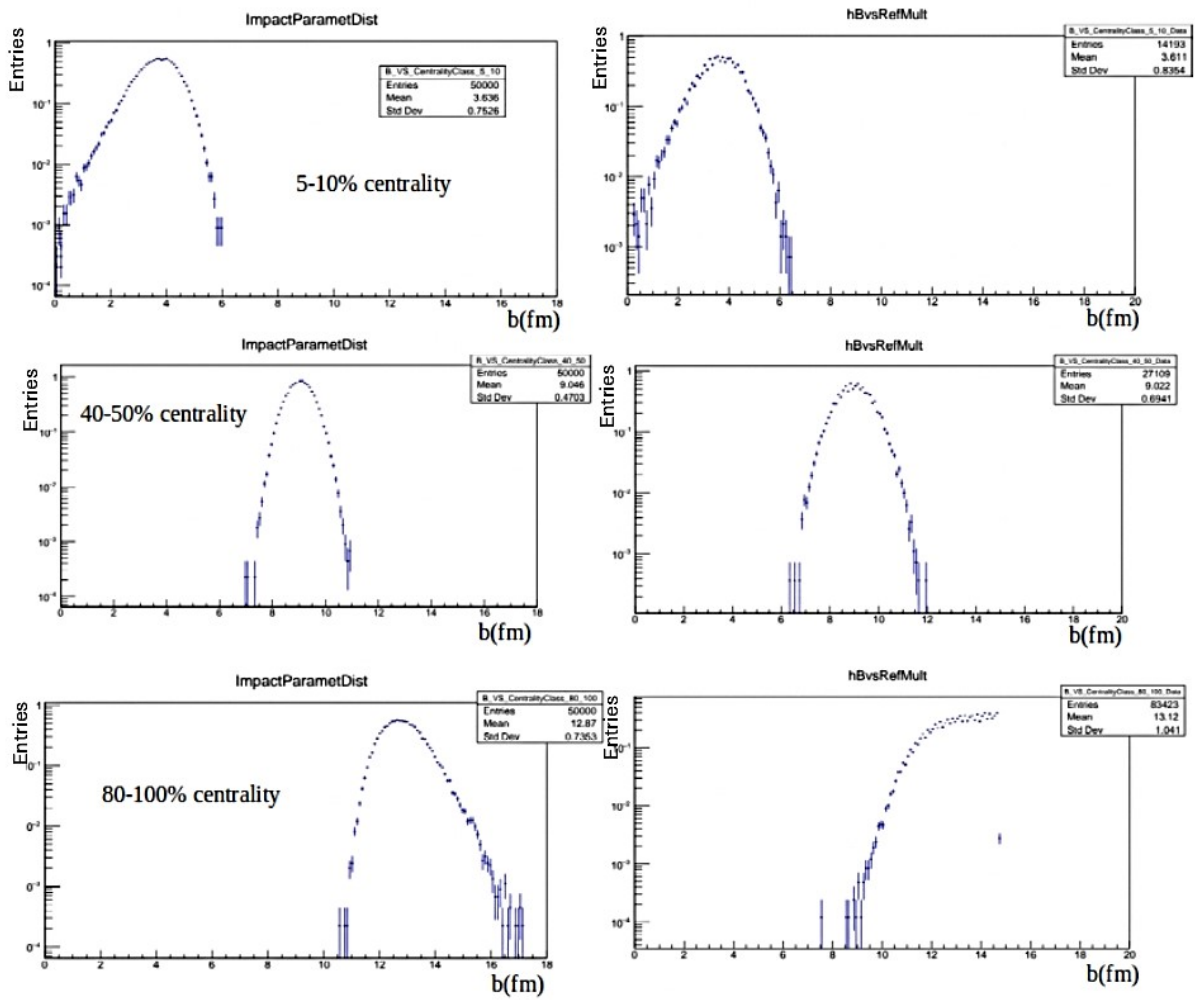


Figure 13: Impact parameter reconstructed by the adjustment and obtained from UrQMD information.

Figure 14 illustrates the ratio in the number of charged particles with respect to the event count as a function of multiplicity. The blue dots represent the data from our input file, while the red dots indicates the fitted curve.

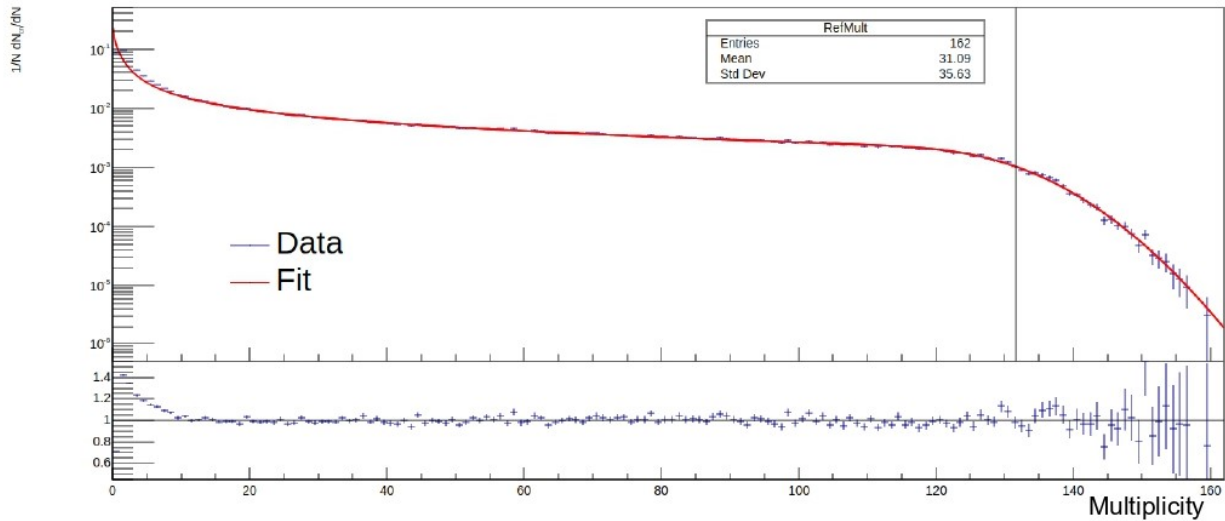


Figure 14: Fit and input file data.

Finally, the impact parameter is extrapolated and compared with the direct one from our UrQMD information, as well as a histogram showing how good the adjustment was presented in figure 15.

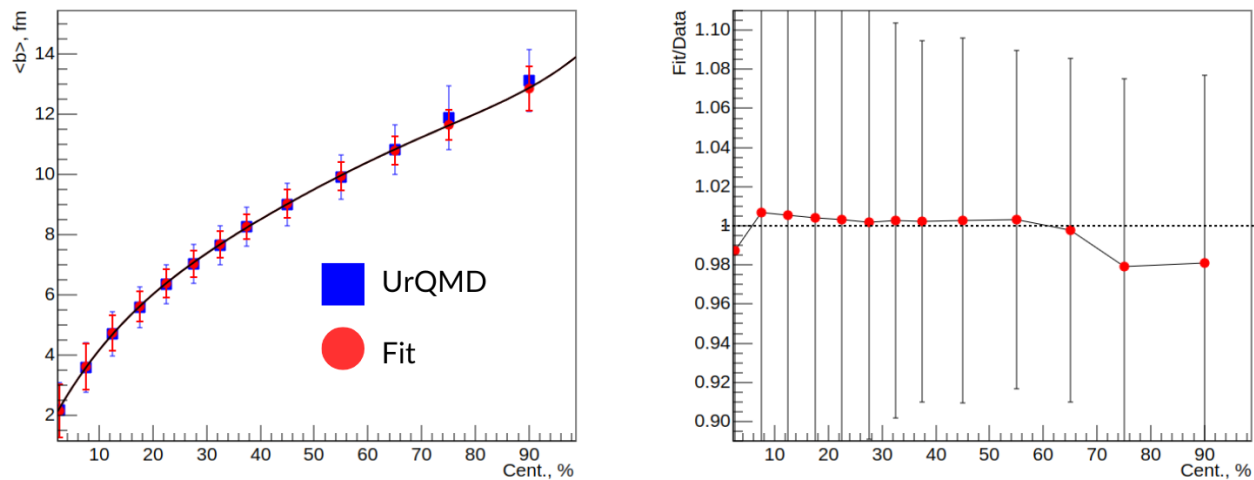


Figure 15: To the left the impact parameter where the red dots are the fit and the blue dots are the data and on the right the ratio of the fit with the data.

In the file ". root" it is also possible to find the different parameters that we could give to configure them, in our case we did not know that the values presented are taken directly from the adjustment, in table 1 are the different parameters that are extracted from the fit, have a sigma that is the total effective section, a theta and nKnee which are variables depending on the collision geometry and different constants $a_{1,2,3}$, as well as the fit error.

Parameter	Value
NDF	143
a1	-3.73
a2	0.164
a3	-2.84
χ^2	163.5
nKnee	131.7
sigma	679.9
teta	0.647
χ^2/NDF	1.143111

Table 1: Centrality, multiplicity and impact parameter data.

With the file "out. C" were extracted the values of centrality and impact parameter presented below in table 2.

Centrality %	Multiplicity	Impact parameter
0-10	162-96	2.94-5.18
10-20	96-70	5.18-6.75
20-30	70-50	6.75-7.39
30-40	50-34	7.39-7.97
40-50	34-23	7.97-9.51
50-60	23-15	9.51-10.42
60-70	15-9	10.42-11.24
70-80	9-5	11.24-12.01
80-100	5-1	12.01-14.10

Table 2: Centrality, multiplicity and impact parameter data.

6.2 Comparison of results

The data of MCGlauber are collected from the work presented in the summer session 2024 of the STAR program entitled "Analysis of the fixed objective mode of the MPD experiment", by the author Adrian Lara Tlaxcala at the following link. https://students.jinr.ru/index.php?session_id=5. The following tables show the data compared for the two methods of centrality, namely multiplicity and impact parameter.

Centrality, %	$N_{chMCglauber}^{min}$	$N_{chMCglauber}^{max}$	$N_{chGammaFit}^{min}$	$N_{chGammaFit}^{max}$	ΔN_{ch}^{min}	ΔN_{ch}^{max}
[0 - 10]	95	164	96	162	1	2
[10 - 20]	70	95	70	96	0	1
[20 - 30]	51	70	50	70	1	0
[30 - 40]	36	51	34	50	2	1
[40 - 50]	24	36	33	34	9	2
[50 - 60]	15	24	15	23	0	1
[60 - 70]	9	15	9	15	0	0
[70 - 80]	5	9	5	9	0	0
[80 - 90]	2	5	1	5	1	0

Table 3: Multiplicities extracted with the two methods and difference between them for different centrality intervals.

Centrality %	$\langle b_{MCglauber} \rangle$	$\langle b_{GammaFit} \rangle$
0-10	2.54	2.21
10-20	4.37	4.7
20-30	5.69	5.62
30-40	6.74	6.4
40-50	7.68	7.68
50-60	8.55	8.24
60-70	9.35	9.02
70-80	10.11	10.84
80-100	10.99	11.63

Table 4: Average impact parameter comparison between methods.

As a comparison, the average of the impact parameters were also plotted as a function of the centrality between the GammaFit method and the MCglauber.

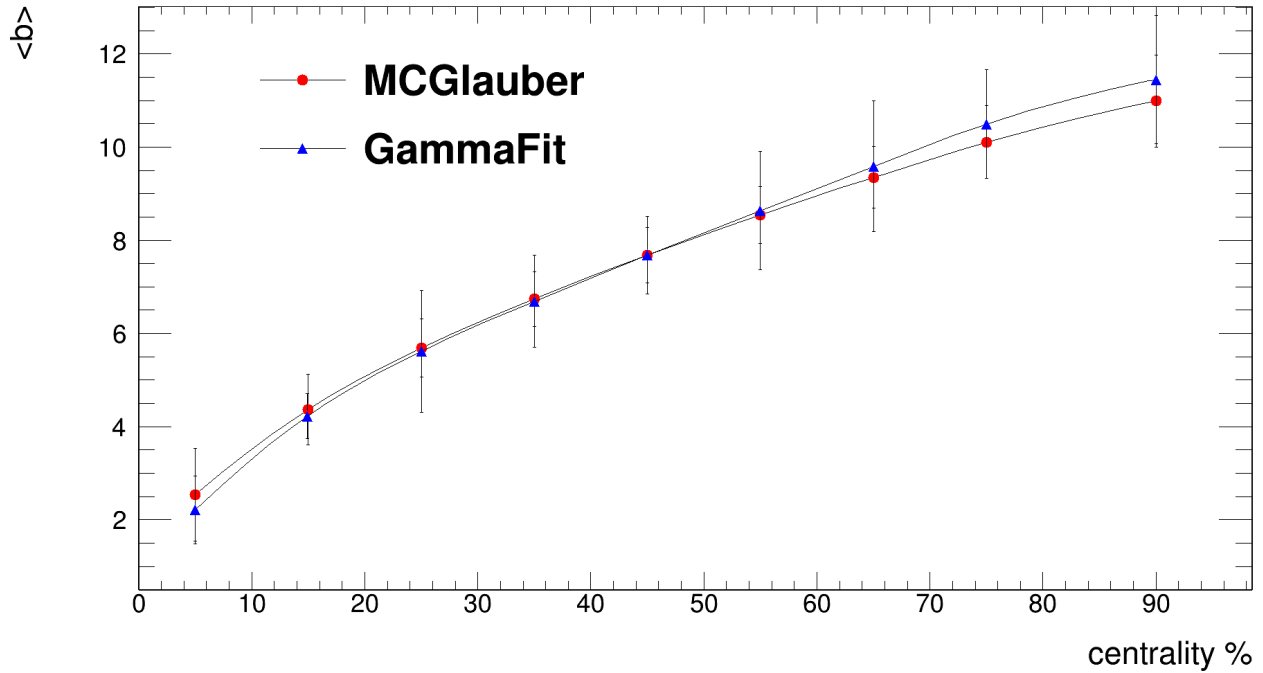


Figure 16: Comparison of the impact parameter between the two different methods.

7 Particle identification

7.1 Energy loss and mass in function the $p \cdot q$

For the identification of particles data were used from the reconstructed ones, to have histograms of loss of energy (dE/dx) as function of the total momentum (p) by the charge (q). If it finds the total distribution you can observe some lines in the histogram in the figure 17 each line belongs to the loss of energy of a different particle, in our case is very notorious the proton and pions, being this the line bigger and marked on the positive side of the X-axis.

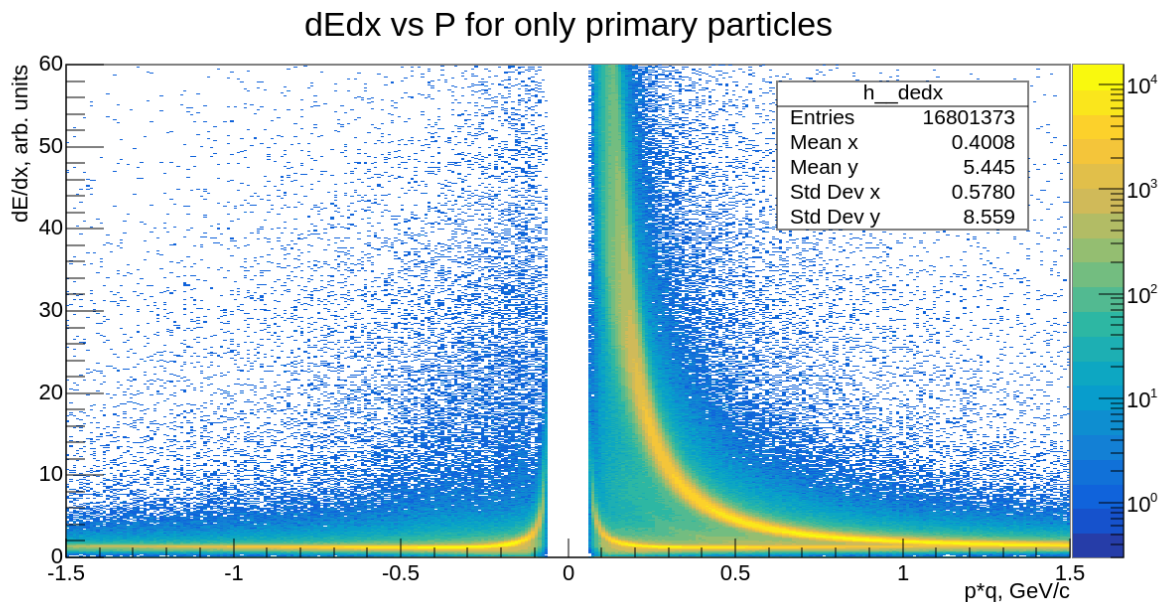


Figure 17: Energy loss distributions for primary particles.

Subsequently, the energy loss distributions were found for different species of particles (π^+ , π^- , K^+ , K^- and p); in order to have a cleaner distribution, the cuts in ($N_{Hits} \geq 20$, $DCA \leq 2$, $\eta \in [-1, 2]$) that are the same for the multiplicity histogram were applied (Figure 11). Figure 18 shows the energy loss distributions by particle species obtained from reconstructed data and MC identification.

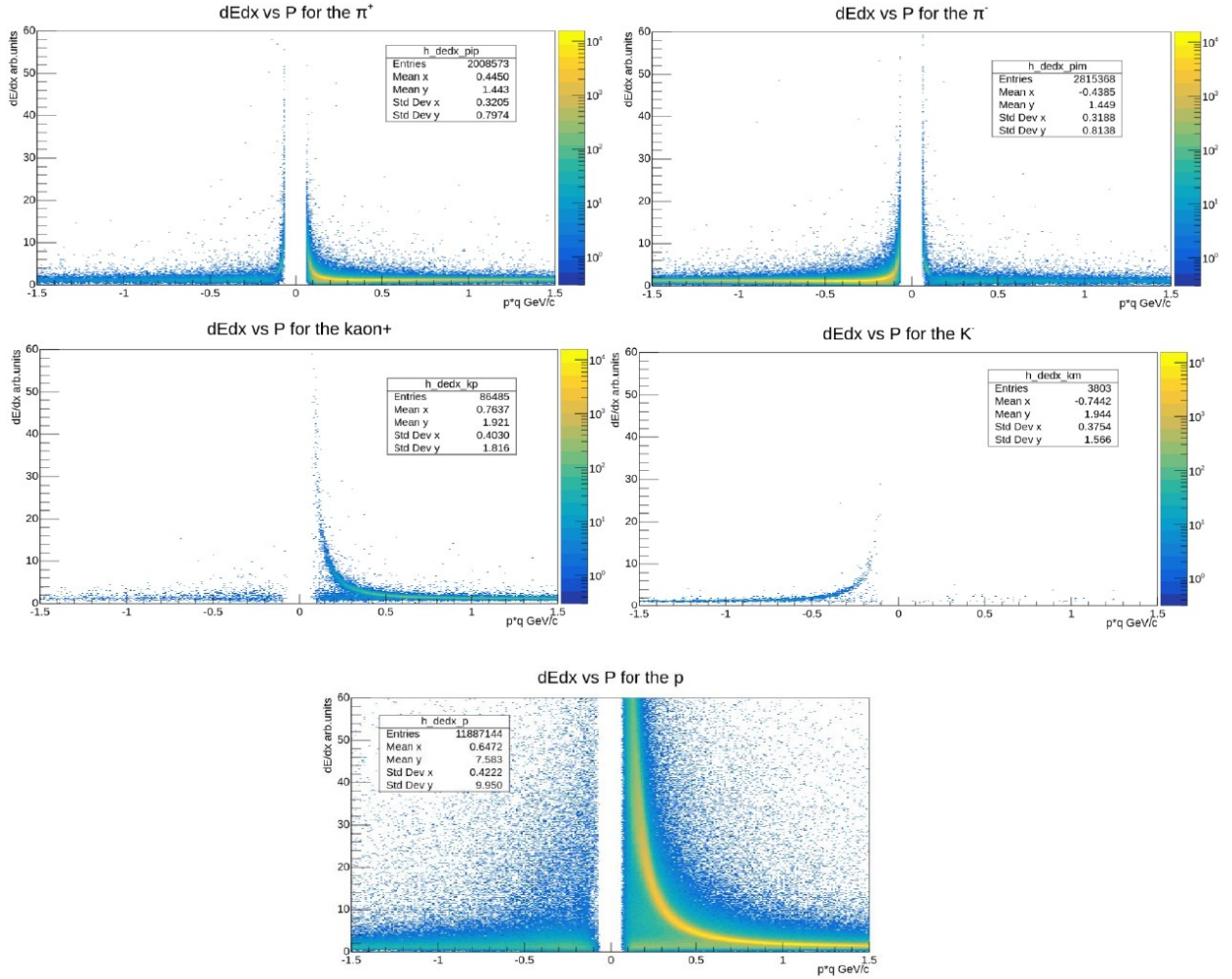


Figure 18: Energy loss distributions by particle species (π^+ , π^- , K^+ , K^- , p).

Mass distributions were also included in the work as p^*q function and histograms were obtained for each different species of particle which are shown in the figure 19. In the same way as for figure 18, MC identification is carried out.

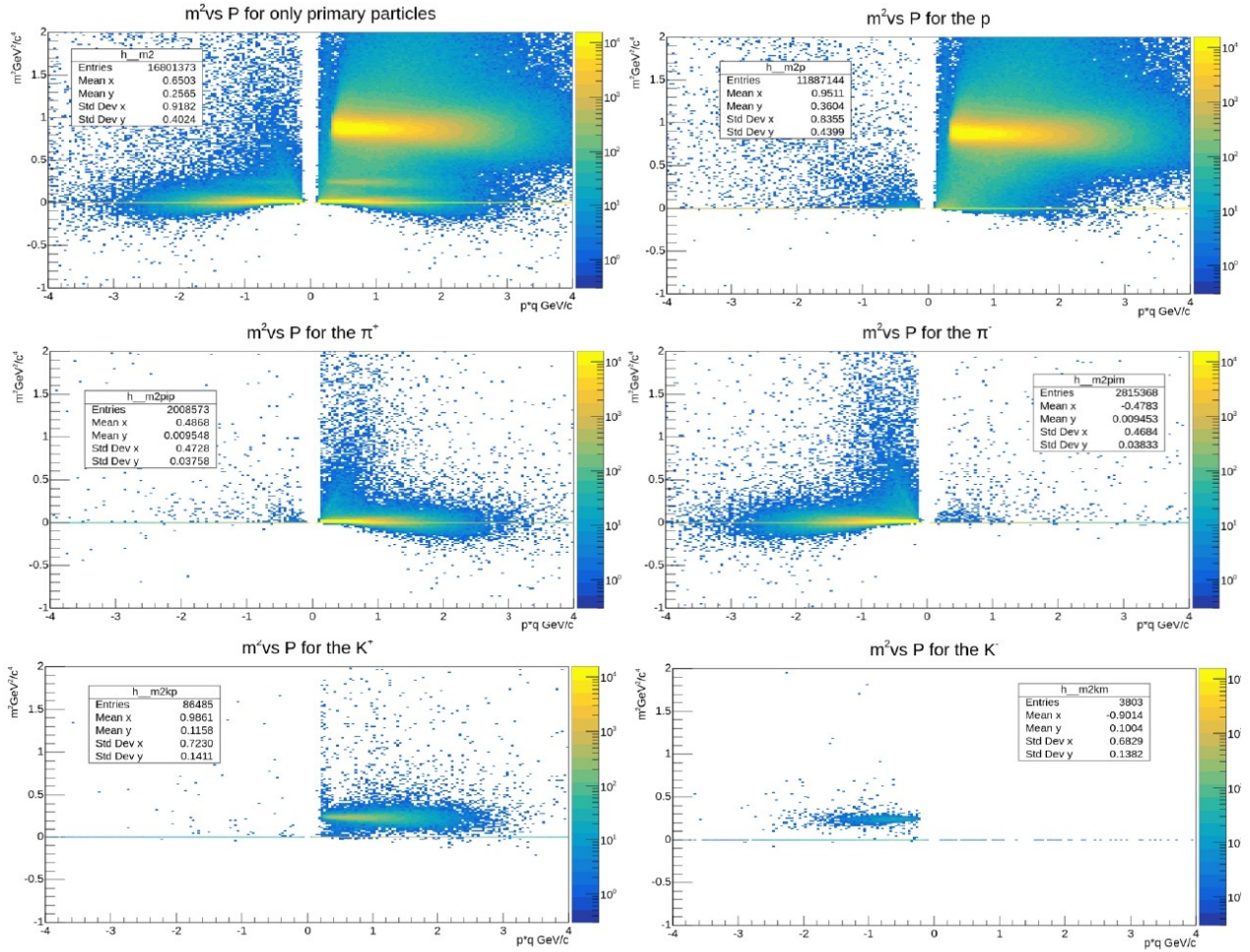


Figure 19: Mass distributions as function of $p \cdot q$ energy by particle species.

7.2 Fit of data

As in reality we will not be able to use ID for the energy loss distributions, as done in the previous section, it is important to describe by adjustments, which is the trend of energy loss, for each specie of particle, so the Bethe-Bloch equation is used, an initial adjustment was given, at the beginning the equation with the parameters that were found on the internet [15], does not describe a good fit, so you have to find again the parameters for the equation. It is important to mention that the settings for energy losses are slightly adjusted but not a good fit. Projections are made on the Y-axis as shown in figure 20:

dE/dx parameterization for the p

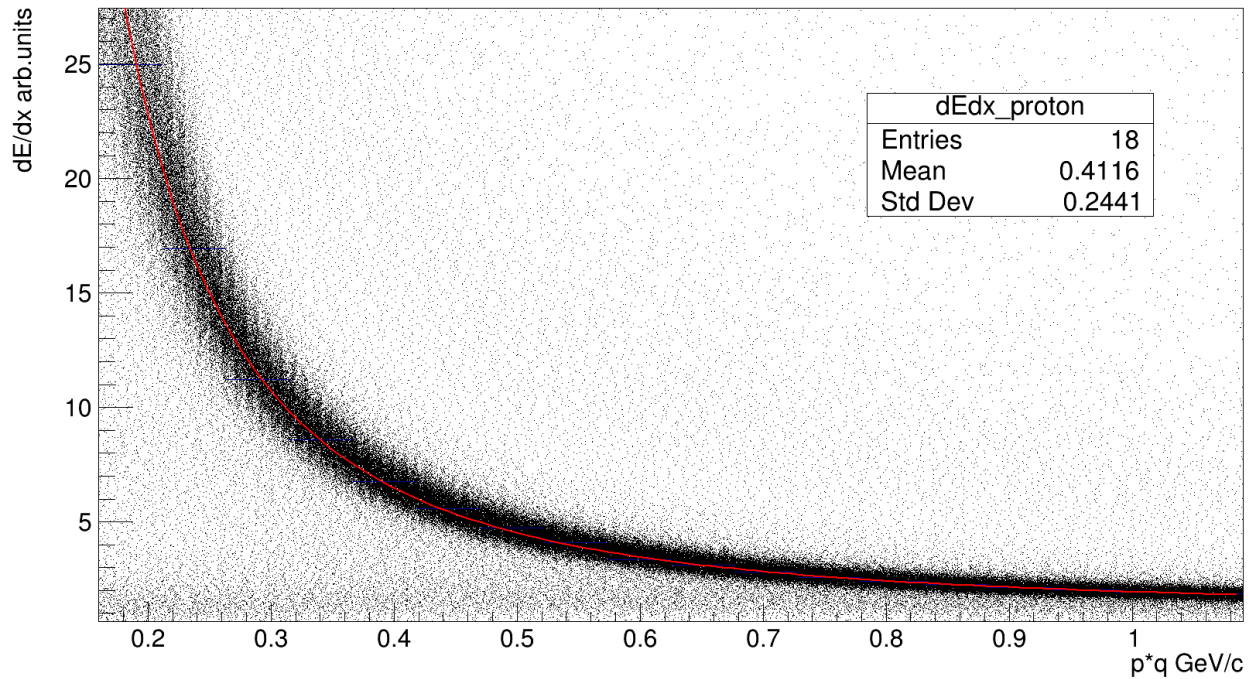


Figure 20: Bethe-Bloch equation adjustment for protons.

For the fit a projection is made on the Y-axis, for the case of protons it was made with slices of 5 bins finding 18 points for adjustment, but for kaon and pion was made with slices of 3 bins but for the pion 16 points were found and for the kaon 12 points for the adjustments. With the projection a gaussian function is adjusted to find the maximum point and a sigma corresponding to the adjustment is separated as shown in figure 21:

dE/dx parameterization for the proton

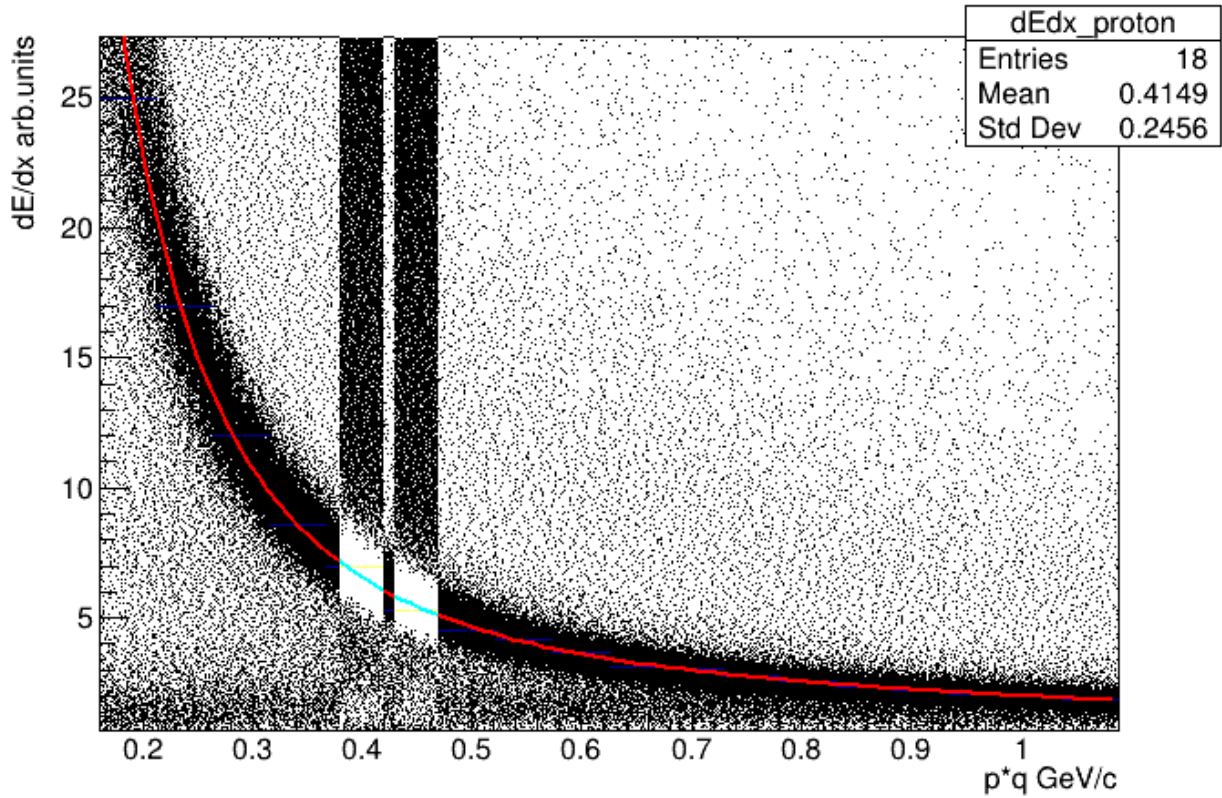


Figure 21: Projection of the Y-axis to find the mean value.

In Figure 22 is the setting of the gaussian used to find the mean value.

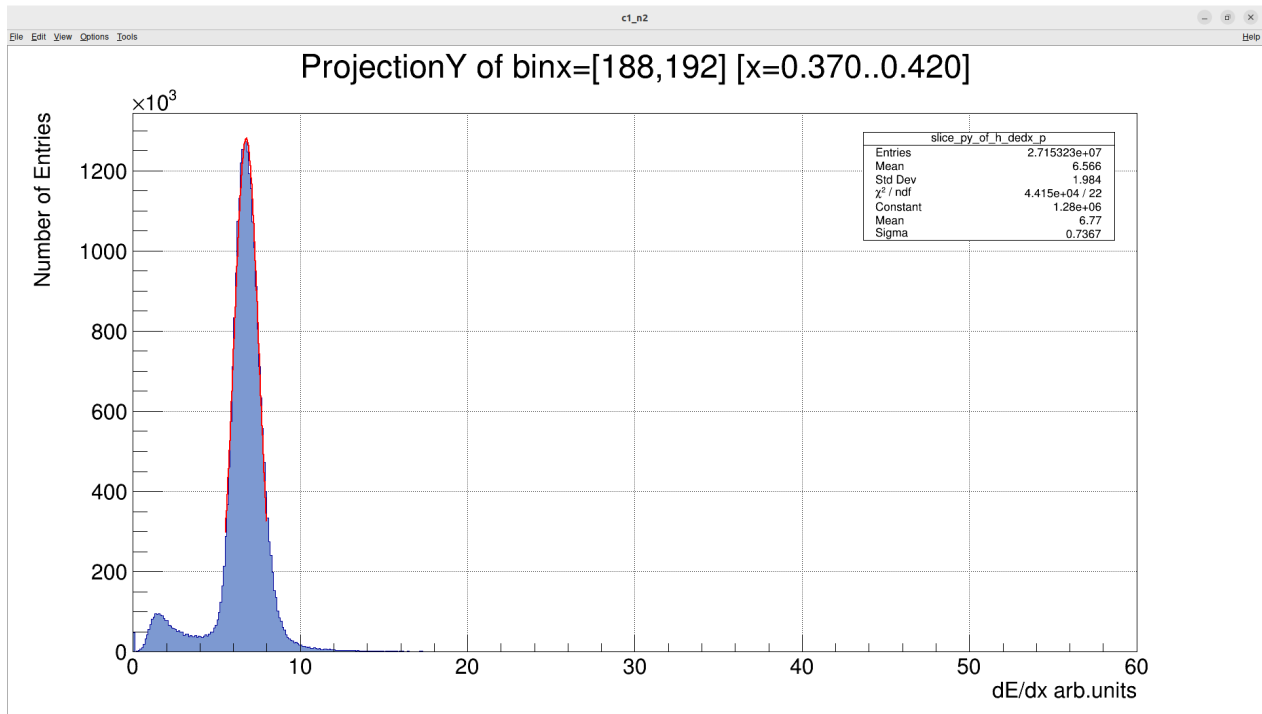


Figure 22: Adjustment with Gaussian function.

The following Table 5 shows the data collected from maximum points and their respective

value of sigma from the fit.

(p) Mean	(p) Sigma	(π^+) Mean	(π^+) Sigma	(K^+) Mean	(K^+)Sigma
24.9622	4.99	2.437	0.4849	4.64478	0.722671
16.941	2.81	1.896	0.2485	3.58656	0.446323
11.236	1.53	1.618	0.1802	2.92935	0.321663
8.582	1.106	1.458	0.1569	2.49404	0.251462
6.7695	0.7367	1.361	0.1412	2.20807	0.223196
5.567	0.5603	1.317	0.1377	1.96815	0.178016
4.723	0.4811	1.262	0.1313	1.80645	0.161765
4.078	0.396	1.239	0.1285	1.68376	0.147452
3.3584	0.3354	1.225	0.1262	1.59043	0.138783
3.119	0.2954	1.219	0.126	1.52035	0.132832
2.8	0.2622	1.215	0.1259	1.46073	0.124656
2.577	0.2419	1.2133	0.1259	1.41887	0.123548
2.39	0.2264	1.2131	0.125		
2.275	0.2168	1.216	0.1267		
2.121	0.1998	1.219	0.1283		
2.016	0.1923	1.224	0.1286		
1.928	0.1853				
1.851	0.1778				

Table 5: Maximum and width point (sigma) of the Gaussian function adjustment.

7.3 Sigma and limits

Once both the maximum point and the sigma of each point of the adjustment are met, every maximum point is added 2 times its sigma to have the maximum limit and twice its sigma to have the minimum limit. With these new values the adjustment was again made to have the values for the Bethe-Bloch equation. Values for each particle species are included in the following tables:

Parameter	π^+ max	π^+ min
p0	-0.694978	-0.4814
p1	-0.5444038	-0.6593
p2	-0.221145	-0.3791
p3	6.0991	6.8815
p4	-0.380694	-0.3162

Table 6: parameters for pions of the Bethe-Bloch equation.

Parameter	K^+ max	K^+ min
p0	-0.954	-1.1444
p1	-0.0273	0.4036
p2	0.8683	1.2918
p3	2.395	1.2918
p4	0.60565	2.9028

Table 7: parameters for kaons of the Bethe-Bloch equation.

Parameter	p max	p min
p0	-1.3055	-1.338
p1	0.3812	0.8953
p2	1.4613	1.955
p3	1.521	0.7643
p4	1.502	2.4008

Table 8: parameters for protons of the Bethe-Bloch equation.

Figure 23 and Figure 24 shows the above-mentioned maximum and minimum adjustment:

dE/dx parameterization for the proton

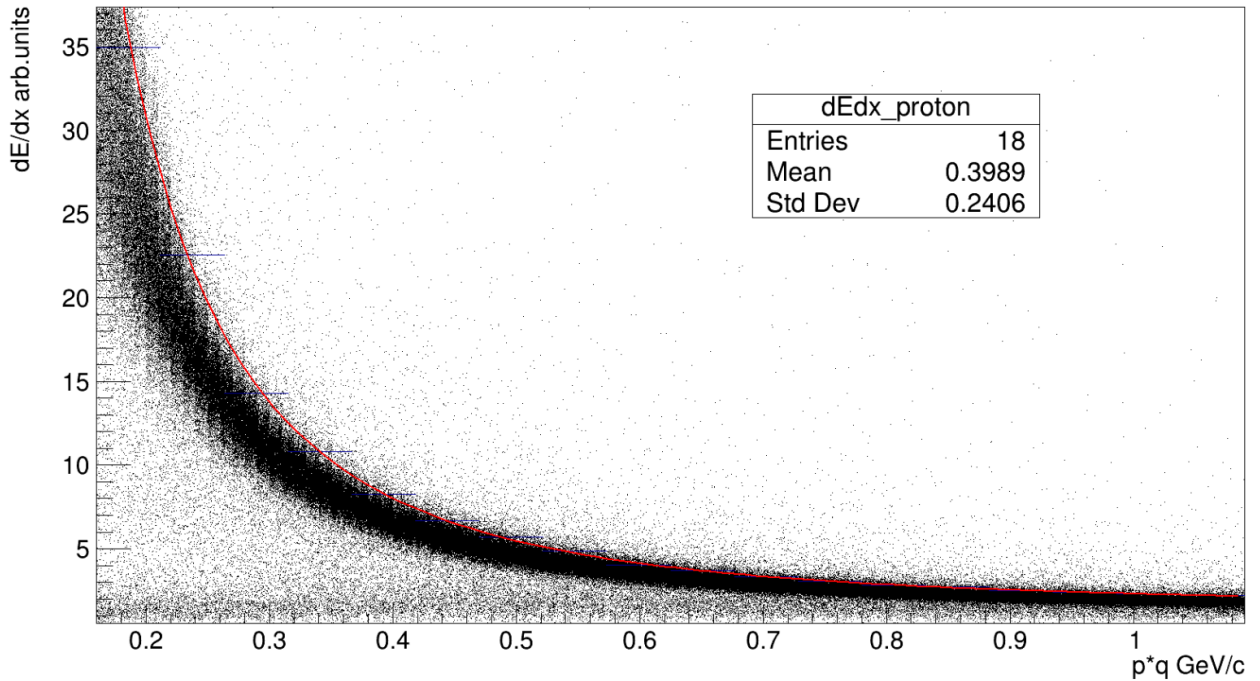


Figure 23: Maximum limit, adding twice the value of sigma to the mean value.

dE/dx parameterization for the p

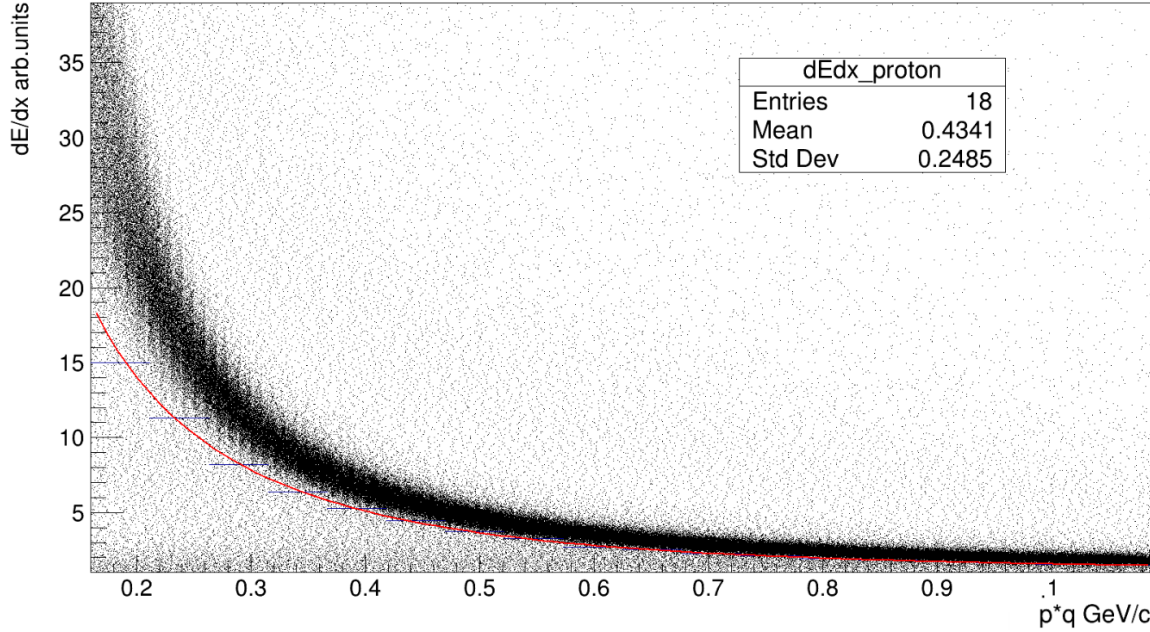


Figure 24: Minimum limit, subtracting the value of sigma twice from the mean value.

The data for maximum and minimum were extended for the particle species we are analyzing (π^+ , K^+ , p). With these limits it is possible to extract their different parameters from the Bethe-Bloch equation and subsequently use them for p_T correction.

7.4 Comparison Fixed Target Mode and Low Magnetic Field

As for the study of reduced magnetic field, particles are being identified, this work includes the comparison between the different adjustments and their maximum and minimum limits chosen from the sigma extracted from the adjustment. The following figures show a comparison between the data analysed in this paper and those of the reduced magnetic field. The data of the reduced magnetic field are reported in the work entitled "Collider Mode (Reduced Magnetic Field). Particle identification determination of spectra using information on energy losses (dE/dx) in TPC and TOF detector Flight-time" that has been presented at the Summer 2025 session of the START program by author Alejandro San Juan on the page https://students.jinr.ru/index.php?session_id=5.

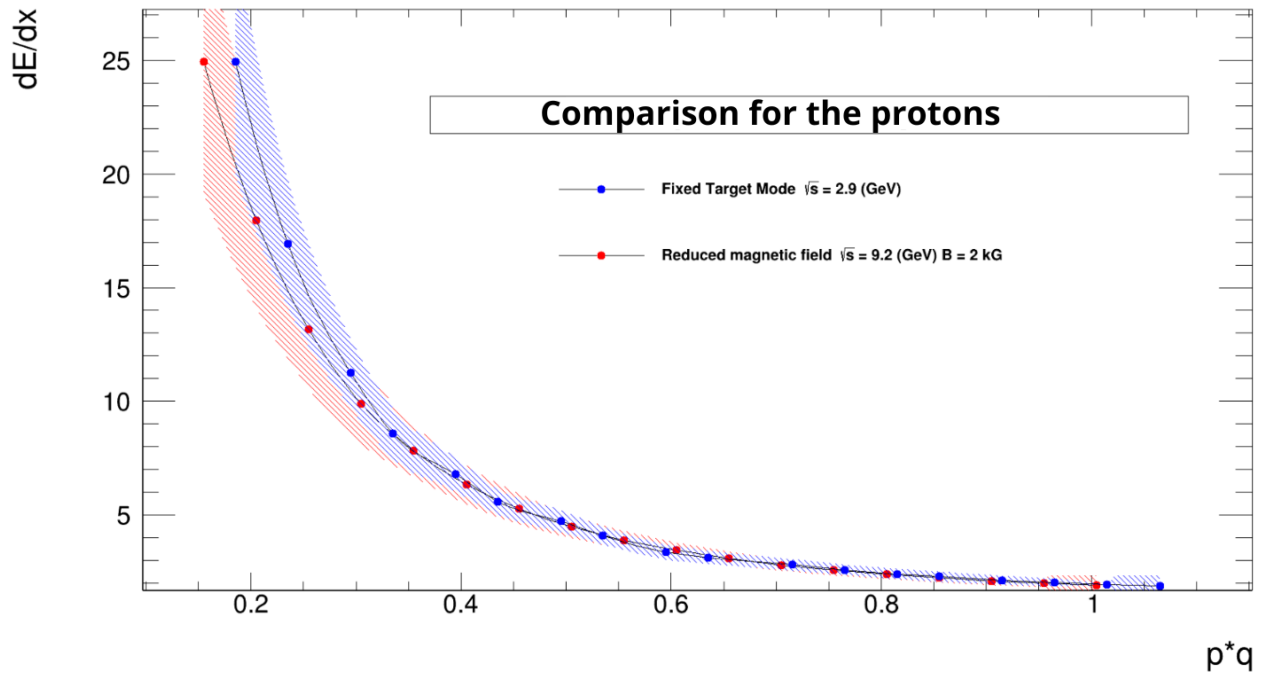


Figure 25: Comparison Fixed Target Mode and Low Magnetic Field for the protons.

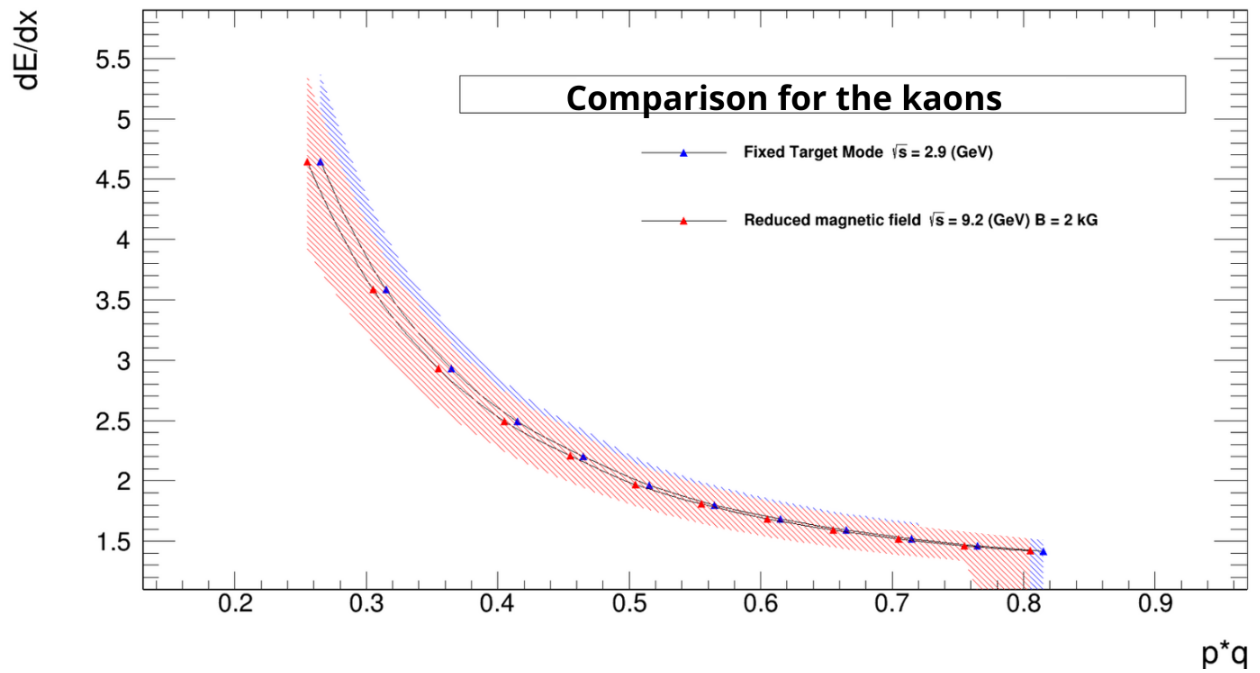


Figure 26: Comparison Fixed Target Mode and Low Magnetic Field for the kaons.

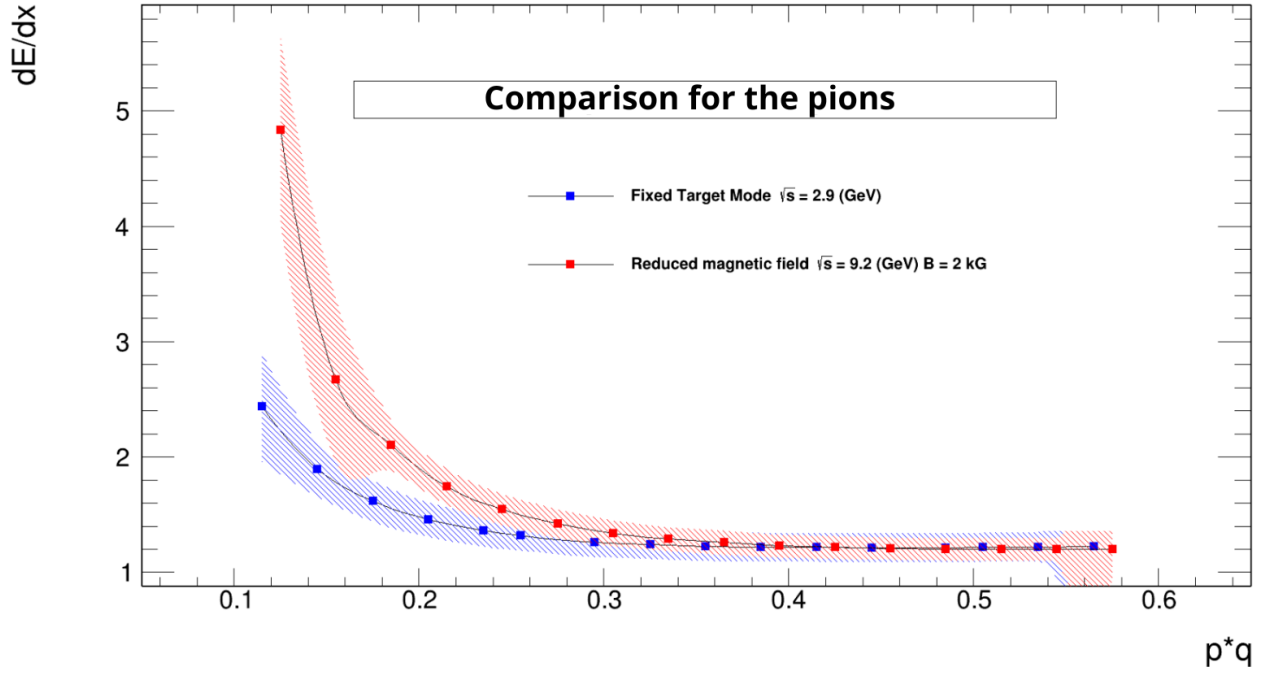


Figure 27: Comparison Fixed Target Mode and Low Magnetic Field for the pions.

As can be seen for the case of pions, there is a greater difference, although for protons and kaons there is not so much difference, if they are described by different settings, so that parameterization must be created both for fixed target mode and for reduced magnetic field. It is important to note that the differences only exist at low p_T because later they follow the same behavior.

7.5 Limits for the dE/dx

The limits above were used to restrict the selection of data, power loss distributions were taken without any selection of the ID MC and the mean values were used with addition or subtraction of the sigma value, also histograms were performed with the limits and with the ID selection to compare the data, the results are shown in the Figure 28 for each particle species.

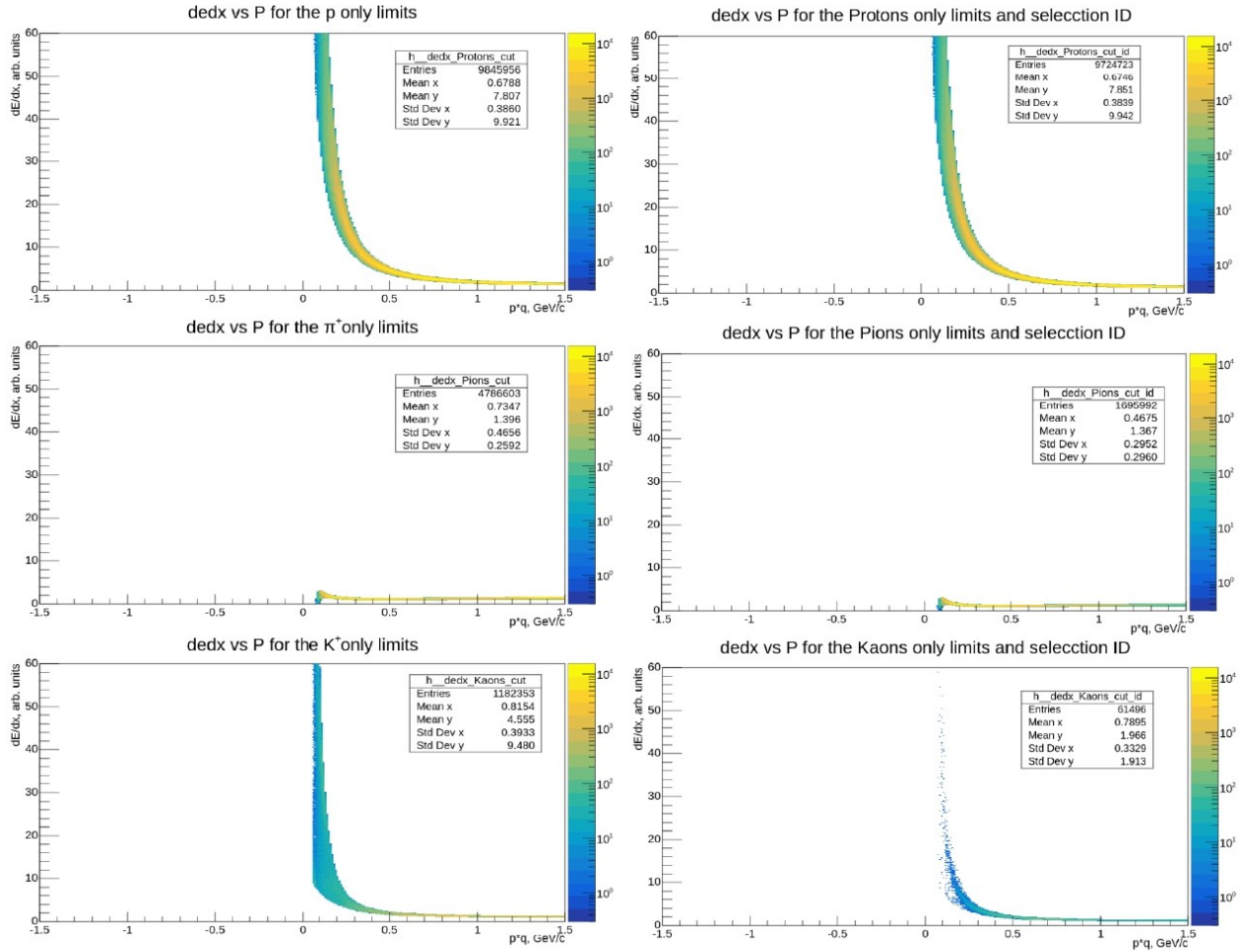


Figure 28: Comparison of energy losses with and without ID selection.

It is also possible to note that for the case of pions and protons the fit is good because when you make the selection of ID to already restricted histograms compared to those that have no selection by ID is not much difference, but for kaons if there is a lot of contamination from particles that are not kaons but are within the cut to a smaller p_T . For example in the case of protons are different in the entrance of particles at 0.012313%, but for the case of kaons is 1.56% different, here we see the difference, means that with the cuts in the selection of kaons is not as good as that of protons because at low momentum there seems to be greater contamination.

7.6 p_T Rec and p_T MC and resolution

Once the cuts were found to be acceptable for the energy loss distributions, the p_T with the cuts was obtained for the reconstructed data, and p_T histograms were also used with Monte Carlo for later comparison. In the following figure we can see a comparison between p_T^{MC} and p_T^{Reco} with PID:

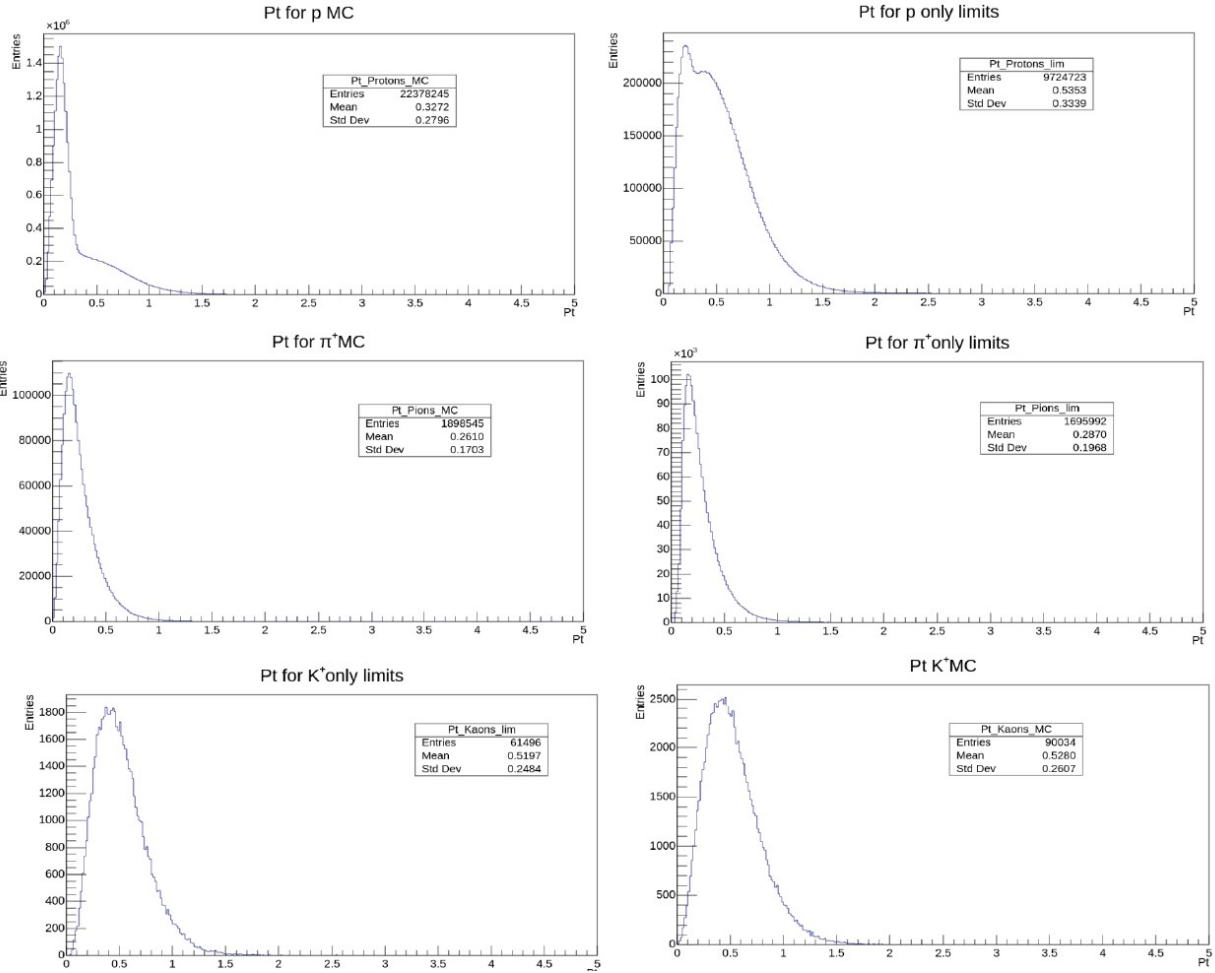


Figure 29: Comparison of p_T^{MC} and p_T^{Reco} selected from the identification of particles.

At the end with the data of p_T is calculated efficiency using both the reconstructed data and the monte carlo, the efficiency was obtained for the different species of particles analyzed (π^+ , K^+ , p) and is found in the following 3 figures.

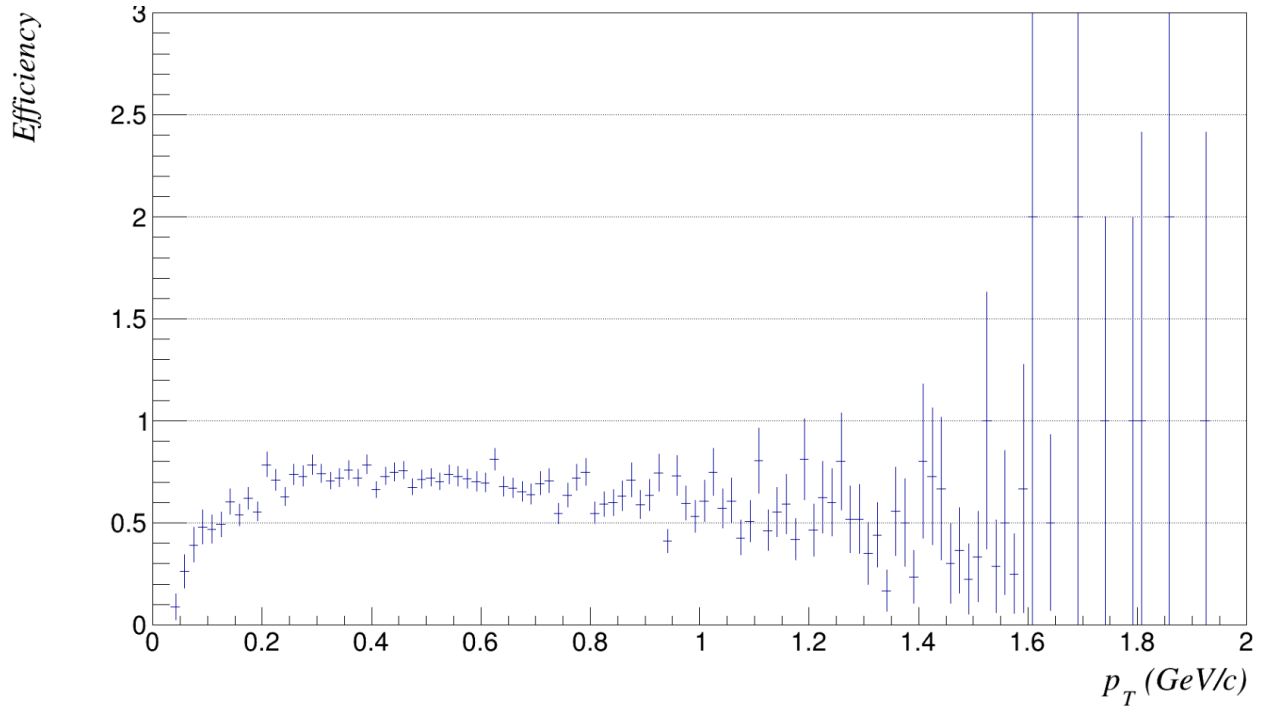


Figure 30: Efficiency for kaons using $Eff = p_T^{Reco} / p_T^{MC}$.

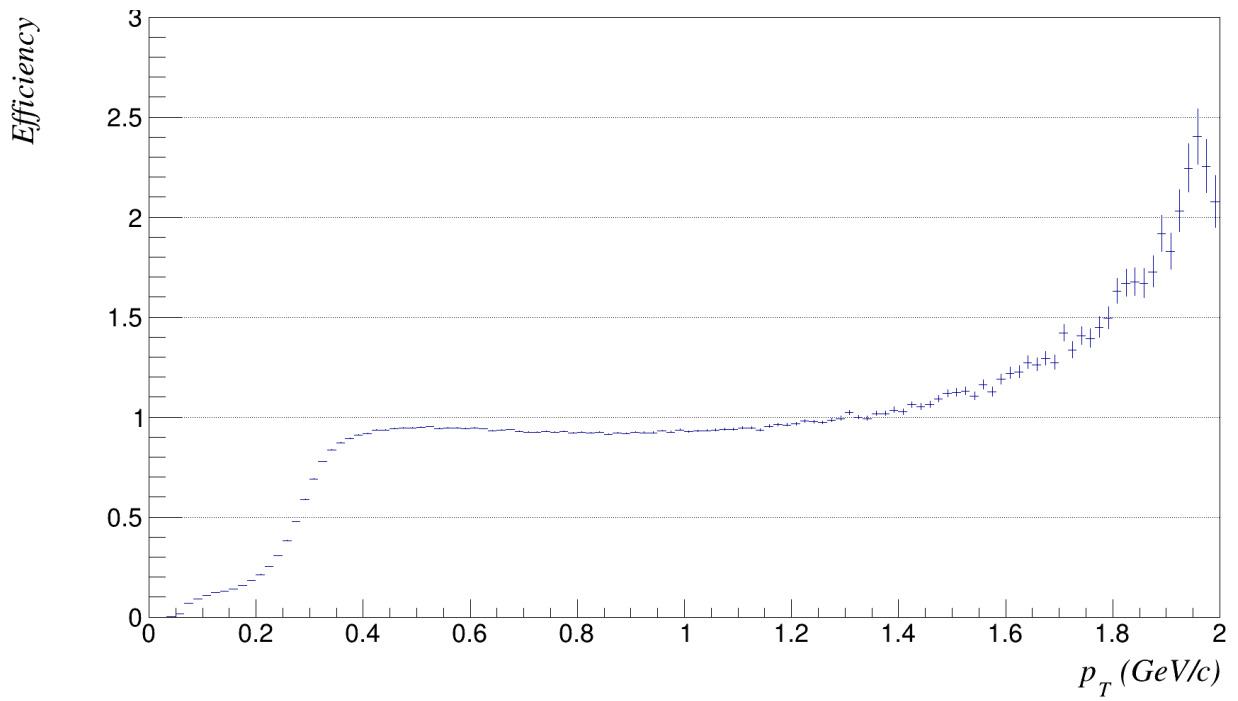


Figure 31: Efficiency for protons using $Eff = p_T^{Reco} / p_T^{MC}$.

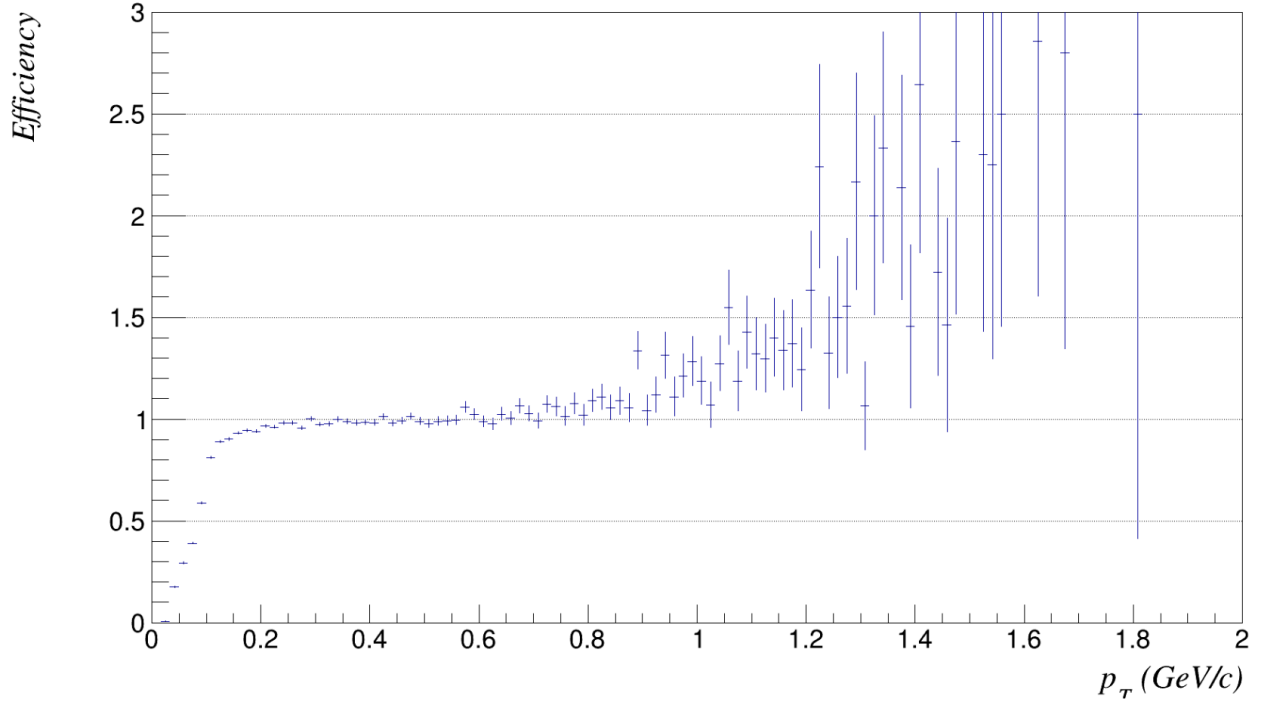


Figure 32: Efficiency for pions using $Eff = p_T^{Reco} / p_T^{MC}$.

It is possible to notice that for pions and protons the efficiency is very good approximately the efficiency is 89.3% for pions and 84.1% for protons, while for the case of kaons the distribution is a little strange since the efficiency is 68.3%. With these results we can see that the identification of particles acceptable but improvements are needed.

8 Conclusions

Different studies were carried out for a series of cuts ($N_{Hits} \geq 20$, $DCA \leq 2$, $\eta \in [-1, 2]$), with the aim of having distributions without much noise, used for multiplicity and energy loss histograms, subsequently made adjustments with Monte Carlo identification to find a series of parameters that adjust the energy loss trend, with these adjustments it was possible to use limits to restrict the reconstructed data and apply them for p_T distributions without the use of MC identification, finally the efficiency of p_T is found to confirm that the identification of particles was so good and in some future it is planned to implement the study for different classes of centrality.

Bibliography

- [1] Peter Parfenov. *Centrality Framework*.
- [2] The NICA LHEP offline computing cluster. Accessed: 2024-07-31.
- [3] Colaboration. Nuclotron-based ion collider facility, 2013. 20-August-2024.
- [4] Colaboration. Multi-purpose detector (mpd), 2013. 20-August-2024.
- [5] Colaboration. Nuclotron, 2013. 20-August-2024.
- [6] Colaboration. 3-d mpd, 2024. 20-August-2024.
- [7] Dr. Marcus Bleicher. Ultrarelativistic quantum molecular dynamics (urqmd), 2013. 20-August-2024.
- [8] Colaboration. The mpdroot, 2024. 20-August-2024.
- [9] Matt Evans. Fixed target vs collider experiments with discussion, 2023. 20-August-2024.
- [10] Braian Adair Maldonado Luna. Cálculo de centralidad en las colisiones de iones pesados con el experimento mpd-nica del jinr, 2022. 20-August-2024.
- [11] Rogly, Giuliano Giacalone, and Jean-Yves Ollitrault. Reconstructing the impact parameter of proton-nucleus and nucleus-nucleus collisions. *Physics Subject Headings*, 98(1):024–902, November 2018.
- [12] A. Mudrokh. Particle identification (pid) and prospects for the study of event-by-event fluctuations at mpd, 2018. 20-August-2024.
- [13] A.Zinchenko. Event reconstruction and physics signal selection in the mpd experiment at nica, 2020. 20-August-2024.
- [14] Jae-Woo Lee. Isoscaling in central sn+sn collisions at 270 mev/u, 2022. 20-August-2024.
- [15] A. Mudrokh. Particle identification (pid) as a tool for the study of event-by-event fluctuations at mpd, 2020. 20-August-2024.
- [16] M. Bleicher et al. Relativistic hadron hadron collisions in the ultrarelativistic quantum molecular dynamics model. *J. Phys. G*, 25:1859–1896, 1999.